Trivalent Actinide Ions Showing Tenfold Coordination in Solution

Patrik Weßling,* Tobias Schenk, Felix Braun, Björn B. Beele, Sascha Trumm, Michael Trumm, Bernd Schimmelpfennig, Dieter Schild, Andreas Geist, and Petra J. Panak

ABSTRACT: Trivalent actinides generally exhibit ninefold coordination in solution. 2,6 Bis(5,6 dipropyl 1,2,4 triazin 3 yl)pyridine (nPr BTP), a tridentate nitrogen donor ligand, is known to form ninefold coordinated 1:3 complexes, $[An(nPr\ BTP)_3]^{3+}$ (An = U, Pu, Am, Cm) in solution. We report a Cm(III) complex with tenfold coordination in solution, $[Cm(nPr\ BTP)_3(NO_3)]^{2+}$. This species was identified using time resolved laser fluorescence spectroscopy (TRLFS), vibronic side band spectroscopy (VSBS), X ray photoelectron spectroscopy (XPS), and density functional theory (DFT). Adding nitrate to a solution of the $[Cm(nPr\ BTP)_3]^{3+}$ complex in 2 propanol shifts the Cm(III) emission band from 613.1 to 617.3 nm. This bathochromic shift is due to a higher coordination number of the Cm(III) ion in solution, in agreement with the formation of the $[Cm(nPr\ BTP)_3(NO_3)]^{2+}$ complex. The formation of this complex exhibits slow kinetics in the range of 5 to 12 days, depending on the water content of the solvent. Formation of a complex $[Cm(nPr\ BTP)_3(X)]^{2+}$ was not observed for anions other than nitrate ($X^- = NO_2^-$, CN^-, or OTf^-). The formation of the $[Cm(nPr\ BTP)_3(NO_3)]^{2+}$ complex was studied as a function of NO_3^- and nPr BTP concentrations, and slope analyses confirmed the addition of one nitrate anion to the $[Cm(nPr\ BTP)_3]^{3+}$ complex. Experiments with varied nPr BTP concentration show that $[Cm(nPr\ BTP)_3(NO_3)]^{2+}$ only forms at nPr BTP concentrations below 10^{-4} mol/L whereas for concentrations greater than 10^{-4} mol/L the formation of the tenfold species is suppressed and $[Cm(nPr\ BTP)_3]^{3+}$ is the only species present. The presence of the tenfold coordinated complex is supported by VSBS, XPS, and DFT calculations. The vibronic side band of the $[Cm(nPr\ BTP)_3(NO_3)]^{2+}$ complex exhibits a nitrate stretching mode not observed in the $[Cm(nPr\ BTP)_3]^{3+}$ complex. Moreover, XPS on $[M(nPr\ BTP)_3(NO_3)](NO_3)_2$ (M = Eu, Am) yields signals from both non coordinated and coordinated nitrate. Finally, DFT calculations reveal that the energetically most favored structure is obtained if the nitrate is positioned on the C_2 axis of the D_3 symmetrical $[Cm(nPr\ BTP)_3]^{3+}$ complex with a bond distance of 413 pm. Combining results from TRLFS, VSBS, XPS, and DFT provides sound evidence for a unique tenfold coordinated Cm(III) complex in solution—a novelty in An(III) solution chemistry.

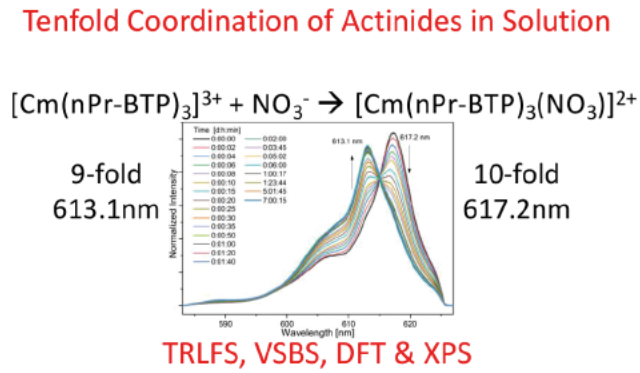

INTRODUCTION

2,6 Bis(5,6 dipropyl 1,2,4 triazin 3 yl)pyridine (nPr BTP, Figure 1) is an extracting agent designed for the separation of trivalent actinides from lanthanides.[1] Its chemistry has been studied extensively over the last 20 years (see reviews[2−5] and references therein). Being a tridentate ligand, nPr BTP forms nine coordinate 1:3 complexes, $[An(nPr\ BTP)_3]^{3+}$ (An = U, Pu, Am, Cm) with trivalent actinides.[6−12] Similar observations were made for lanthanides.[6−8,11−17]

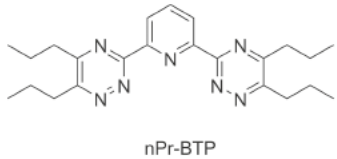

Figure 1. Molecular structure of nPr BTP.

The light trivalent lanthanides show ninefold coordination in solution while the heavy lanthanides are coordinated eightfold. An equilibrium between the coordination numbers (CN) eight and nine is found for the intermediate trivalent lanthanides.[18−24] The reduction in CN is due to the lanthanide contraction. A similar trend is observed for trivalent actinide ions, with the transition from CN = 9 to CN = 8 for Cm(III)−Cf(III).[25] Yet, CN greater than nine are published for trivalent lanthanides[26,27] and actinides[23,28−31] in solution.

Table 1 gives an overview of published CN for trivalent actinide ions in solution determined by extended X ray

absorption fine structure spectroscopy (EXAFS), NMR, or TRLFS.

Table 1. Overview of Coordination Numbers (CN) of Trivalent Actinides in Solution

	An(III)
U	9[8,31,32,a]
Np	9,[31,a,33,a] 10[31,a]
Pu	8,[34,a] 9,[9,23,35,a] 10[29,31,a]
Am	9,[8,a,36,37,b,10,38,39,c] 10,[23,a] 11[30,b]
Cm	8,[40,b] 9,[7,a,40−43,b] 10[23,a,28,b]

[a]Determined by EXAFS. Error of CN 10−20%.[29,31,44,45] [b]Determined by TRLFS. Error of CN ± 0.5.[41,42] [c]Determined by ^{1}H NMR.

Most of the published CN ≥ 10 were determined by EXAFS. Due to the error in CN (±10−20%) obtained by EXAFS measurements and the conclusions described by the authors,[29,31,44,45] further techniques are needed to provide unambiguous evidence for the existence of trivalent actinide species with CN ≥ 10 in solution.

The hydration of Am(III) in aqueous solution was studied by TRLFS. CN = 11 was concluded from the fluorescence lifetime, τ_{Am} = (20.4 ± 2.1) ns[30,37] The stated uncertainty in lifetime measurement results in a range of 9.9 < CN < 12.6, and the paper states that the high CN "may be caused by the short lifetime of the Am(III) species and the limitations of the spectroscopic equipment."

The complexation of Cm(III) with triethylenetetramine *N,N,N′,N″,N‴,N′′′* hexaacetic acid (TTHA) was studied by TRLFS.[28] Tenfold coordination without water in the first coordination sphere was concluded from the Cm(III) fluorescence lifetime of τ_{Cm} = 602 μs and a debatable tenfold denticity of TTHA.[37,46] However, later publications report shorter florescence lifetimes corresponding to one inner sphere water molecule.[37,41]

To provide more evidence for a trivalent actinide species with CN ≥ 9 in solution, the complexation of Cm(III) with nPr BTP in the presence of nitrate was thoroughly studied using TRLFS, vibronic side band spectroscopy (VSBS), density functional theory (DFT), and X ray photoelectron spectros copy (XPS). The formation of a presumed tenfold coordinated species was studied as a function of time and as a function of the nitrate and nPr BTP concentrations. Furthermore, the question was addressed whether an analogous species would form in the presence of other small anions (NO_2^-, CN^-, OTf^-).

EXPERIMENTAL SECTION

Chemicals. Caution! ^{248}Cm and ^{243}Am are α emitters. They have to be handled in dedicated facilities with appropriate equipment for radioactive materials to avoid health risks caused by radiation exposure.

All commercially available chemicals (Alfa Aesar or Sigma Aldrich) used in this study were analytical reagent grade and used without further purification. nPr BTP was synthesized according to the literature.[47]

TRLFS Sample Preparation. A Cm(III) stock solution (2.12 × 10^{-5} mol/L $Cm(ClO_4)_3$ in 0.1 mol/L $HClO_4$; ^{248}Cm: 89.7%, ^{246}Cm: 9.4%, ^{243}Cm: 0.4%, ^{244}Cm: 0.3%, ^{245}Cm: 0.1%, ^{247}Cm: 0.1%) was used for preparing the Cm(III) samples. Tetrabutylammonium nitrate (TBAN) was used as an organic nitrate salt. To perform experiments in the absence of water, aliquots of the Cm(III) stock solution were evaporated at 80 °C for 20 min before adding the organic solvent. The starting volume of each sample was 1 mL.

For experiments in dependence of the nitrate concentration and constant nPr BTP concentration, a 1 × 10^{-2} mol/L TBAN solution was prepared by dissolving 6.08 mg in 2 mL 2 propanol. A 1 × 10^{-3} mol/L nPr BTP solution was prepared by dissolving 1.23 mg in 2 mL of 2 propanol. Samples were prepared by adding 4.7 μL Cm(III) stock solution to the required volumes of TBAN and nPr BTP solutions, 2 propanol, and, if needed, water. The resulting initial Cm(III) concentration was 1 × 10^{-7} mol/L. Samples were stored under 2 propanol atmosphere to avoid evaporation of the solvent over time.

For experiments in dependence of the nPr BTP concentration at constant anion concentrations (NO_3^-, NO_2^-, CN^-, OTf^-), stock solutions of the different anions were prepared: 2.0 mg of KCN dissolved in 10 mL of methanol, 2.0 mg of NaOTf in 10 mL of methanol, and 3.0 mg of $NaNO_2$ in 5 mL of ethanol. In the case of nitrate the TBAN solution (described above) was used. A 1 × 10^{-3} mol/L nPr BTP solution was prepared by dissolving 1.23 mg in 2 mL of the solvent containing 2 × 10^{-5} mol/L of the respective anion. 9.44 μL of the Cm(III) stock solution were evaporated, and aliquots of the KCN, NaOTF, $NaNO_2$, or TBAN solutions were added to yield anion concentrations of 2 × 10^{-5} mol/L and an initial Cm(III) concentration of 2 × 10^{-7} mol/L. Aliquots of the nPr BTP solution were added.

TRLFS Measurements. TRLFS measurements in the presence of various anions (NO_3^-, NO_2^-, CN^-, OTf^-) were performed using an excimer pumped dye laser system (Lambda Physics 201 and FL 3002). The fluorescence emission was detected by an optical multichannel analyzer consisting of a polychromator (Jobin Yvon, HR 320) with a 1200 lines/mm grating and an intensified photodiode array (Spectroscopic Instruments, ST 180, IRY700G).

All other measurements were performed with a Nd:YAG (Surelite II laser, Continuum) pumped dye laser system (NarrowScan D R; Radiant Dyes Laser Accessories GmbH). A spectrograph (Shamrock 303i, ANDOR) with a 1199 lines per mm grating was used for spectral decomposition. The fluorescence emission was detected by an ICCD camera (iStar Gen III, ANDOR).

All measurements were performed at 298 K. A wavelength of 396.6 nm was used to excite Cm(III). The fluorescence was detected after a delay time of 1 μs to discriminate short lived organic fluorescence and light scattering.

VSBS Measurements. Samples for VSBS were 1 × 10^{-7} mol/L Cm(III) with 2.23 × 10^{-5} mol/L nPr BTP in 2 propanol and 1 × 10^{-7} mol/L Cm(III) with 1.6 × 10^{-5} mol/L nPr BTP and 1 × 10^{-4} mol/L TBAN in 2 propanol with 2.5 vol % H_2O. The latter sample contained 64% $[Cm(nPr\ BTP)_3(NO_3)]^{2+}$ as determined by peak deconvolution. Vibronic side band (VSB) spectra were recorded with a 1199 lines per mm grating in the range of 645−800 nm.

XPS Measurements. For XPS analyses a PHI model 5600ci (Physical Electronics Inc.) was used. To achieve high energy resolution of the elemental lines and to minimize sample alteration during the measurements, monochromatic Al K_α X ray excitation (1486.7 eV) at a source power of 50 W was used. The angle of emission (sample normal to analyzer) was set to 25°. The pass energy of the electron analyzer was 11.75 eV, and the step size was 0.1 eV/step. At these conditions, the FWHM of the Ag $3d_{5/2}$ elemental line is 0.61 eV. The binding energy scale of the spectrometer was calibrated according to published binding energies[48] using Cu $2p_{3/2}$, Ag $3d_{5/2}$, and Au $4f_{7/2}$ elemental lines of sputter cleaned pure metal foils. The error in binding energy is estimated to be within 0.2 eV. As a charge reference, the maximum of the C 1s spectrum assigned to the aliphatic carbon atoms of the propyl chains was set to 284.8 eV. Spectra were analyzed by the use of PHI MultiPak software.

nPr BTP/HNO_3 Sample: 130 μL of 0.15 mol/L HNO_3 was evaporated to almost dryness and dissolved in 170 μL of 3 × 10^{-3} mol/L nPr BTP in 2 propanol.

Eu(III)/nPr-BTP Samples. Solutions of 1 × 10^{-3} mol/L Eu(III) and 3 × 10^{-3} mol/L nPr BTP in 2 propanol were prepared by dissolving $Eu(NO_3)_3 \cdot 6\ H_2O$ and nPr BTP in 2 propanol.

Eu(III)/nPr-BTP/HNO_3 Samples. Ten microliters of 1.7×10^{-2} mol/L $Eu(NO_3)_3$ in 0.5 mol/L HNO_3 was added to 100 μL of 0.15 or 0.5 mol/L HNO_3. The solutions were evaporated to almost dryness. 170 μL of 3×10^{-3} mol/L nPr BTP in 2 propanol was added, resulting in solutions of 1×10^{-3} mol/L Eu(III)/nPr BTP 1:3 complex.

Am(III)/nPr-BTP Sample. Ten microliters of 1.7×10^{-2} mol/L $^{243}Am(III)$ in approximately 0.5 mol/L HNO_3 was added to 100 μL of 0.15 mol/L HNO_3. The solution was evaporated to almost dryness. 170 μL of 3×10^{-3} mol/L nPr BTP in 2 propanol was added, resulting in a solution of 1×10^{-3} mol/L Am(III)/nPr BTP 1:3 complex.

One microliter of each of the prepared solutions was spread onto aluminum foil (UHV aluminum foil, All Foils, Inc.), and the solvent was evaporated under air. This resulted in a thin film of approximately 5 mm in diameter, which was analyzed by XPS.

Quantum Chemical Calculations. A four step approach was performed (see Figure 2) using the TURBOMOLE[49] software

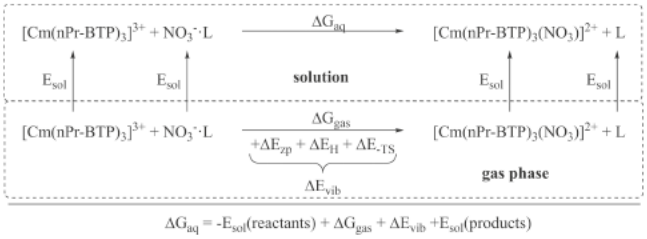

Figure 2. Calculation of the free enthalpy in solution ΔG_{aq} for the formation of $[Cm(nPr\ BTP)_3(NO_3)]^{2+}$ from optimized gas phase structures according to Hess' law.

package to confirm the experimental results. First, structure optimizations using density functional theory (DFT) with the BP86[50,51] functional and def SV(P)[52] basis sets were performed. In all calculations, Cm(III) was described by the ECP60MWB[53] small core pseudopotential and corresponding basis sets of triple ζ quality. By computation of vibrational modes, energetic minima as well as the thermodynamic corrections $E_{vib} = E_{zp} + E_H + E_{-TS}$, with E_{zp}, E_H, and E_{-TS} corresponding to zero point energy, enthalpy, and entropy corrections, respectively, were obtained. Four energy minima were found and reoptimized in the second step on the B3 LYP[54]/def2 TZVP[55] level to achieve more accurate structures. In the third step, electron correlation was added by Møller−Plesset perturbation theory (MP2) calculations to determine accurate ground state energies E_0. Finally, solvent interactions E_{sol} were accounted for by COSMO[56] calculations ($\varepsilon_{2\text{-propanol}} = 18$, $r_{Cm} = 192$ pm).

Computation of VSB Spectra. In order to compare computed vibrational intensities and VSBS data, all calculated modes were scaled by r^{-6} with r being the atomic distance to the Cm(III) atom. Gaussian line broadening was used on calculated frequencies and intensities to obtain VSB spectra.

RESULTS AND DISCUSSION

Kinetic Studies. The evolution of the Cm(III) emission spectra after addition of nitrate to a solution of $[Cm(nPr\ BTP)_3]^{3+}$ was studied as a function of time. Cm(III) emission spectra resulting from the $^6D'_{7/2} \rightarrow {}^8S'_{7/2}$ transition are shown in Figure 3.

A Cm(III) emission band at 617.2 nm with a hot band at 606 nm was detected directly after the addition of nitrate (t = 0). Within the first hour, this emission band decreased and a new emission band at 613.1 nm with a hot band at 605 nm evolved. This evolution of the Cm(III) fluorescence spectra continued for 5 days. For longer periods of time no further change of the Cm(III) emission spectra was detected.

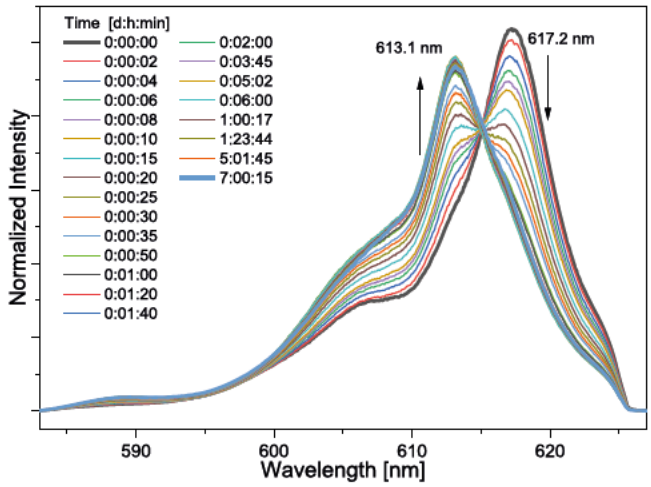

Figure 3. Normalized Cm(III) emission spectra in 2 propanol as a function of time after the addition of nitrate. $[Cm(III)]_{ini} = 1 \times 10^{-7}$ mol/L; [nPr BTP] = 1.58×10^{-5} mol/L; [TBAN] = 4.03×10^{-5} mol/L.

The emission band at 613.1 nm is in excellent agreement with published emission spectra of $[Cm(nPr\ BTP)_3]^{3+}$.[11,57,58] The emission band at 617.2 nm, however, is so far unknown. The bathochromic shift of 4.1 nm is due to a stronger ligand field splitting of the $^6D''_{7/2}$ state of Cm(III) and points to the coordination of an additional ligand in the first coordination sphere.

Nitrate anions are known to be comparably weak ligands in aqueous solutions[59] but can form inner sphere complexes with trivalent actinides and lanthanides at higher nitrate concentrations.[60] In many nonaqueous solutions nitrate anions exhibit strong complexation properties due to lacking competition with water.[61,62] Consequently, the emission band at 617.2 nm belongs to the $[Cm(nPr\ BTP)_3(NO_3)]^{2+}$ complex.

To study the influence of water on the formation of $[Cm(nPr\ BTP)_3(NO_3)]^{2+}$, kinetic experiments were performed in 2 propanol containing 2.5 and 5 vol % H_2O. The Cm(III) emission spectra as a function of time after the addition of nitrate are shown in the SI, Figure S1. In contrast to the sample without water, the emission band of $[Cm(nPr\ BTP)_3]^{3+}$ was exclusively observed directly after addition of nitrate. However, a shoulder at 616.1 nm evolved in both water containing samples over the course of several days. In the sample containing 2.5 vol % H_2O no further changes of the Cm(III) emission spectra were observed after 11 days, indicating that the chemical equilibrium was reached. It took 12 days to attain equilibrium in the case of the sample containing 5 vol % H_2O.

Single component spectra of $[Cm(nPr\ BTP)_3(NO_3)]^{2+}$ in the different solvents were derived by peak deconvolution. They are shown in Figure 4 and compared to the spectrum of the $[Cm(nPr\ BTP)_3]^{3+}$ complex.

The emission spectra of $[Cm(nPr\ BTP)_3(NO_3)]^{2+}$ in the presence of 2.5 and 5% vol % H_2O water are similar, with maxima at 616.4 nm (2.5 vol % H_2O) and 616.3 nm (5 vol % H_2O) and two hot bands at 610 and 599 nm. Thus, the concentration of water in the solvent does not influence the fluorescence emission of $[Cm(nPr\ BTP)_3(NO_3)]^{2+}$. The emission spectrum in pure 2 propanol shows a slight bathochromic shift to 617.3 nm and one hot band at 606 nm.

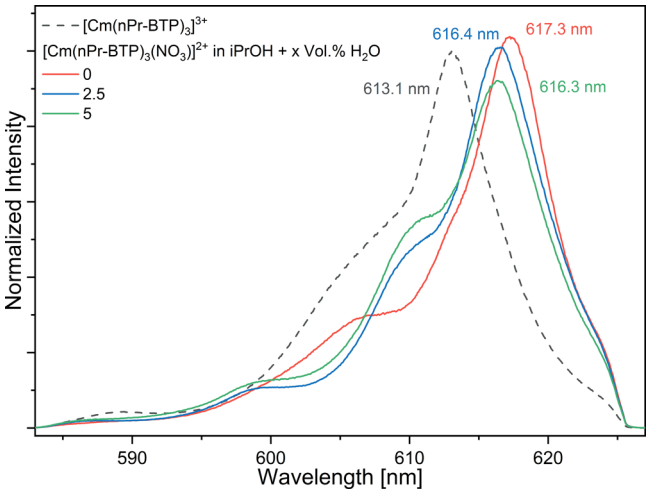

Figure 4. Single component spectra of $[Cm(nPr\ BTP)_3]^{3+}$ and $[Cm(nPr\ BTP)_3(NO_3)]^{2+}$ in 2 propanol containing 0, 2.5, and 5 vol % H_2O.

The single component spectra were used to deconvolute the kinetic series of spectra and to obtain molar fractions of $[Cm(nPr\ BTP)_3(NO_3)]^{2+}$ as a function of time. An example for peak deconvolution is given in the SI, Figure S2. The temporal evolution of the molar fraction of $[Cm(nPr\ BTP)_3(NO_3)]^{2+}$ in the different solvents is shown in Figure 5.

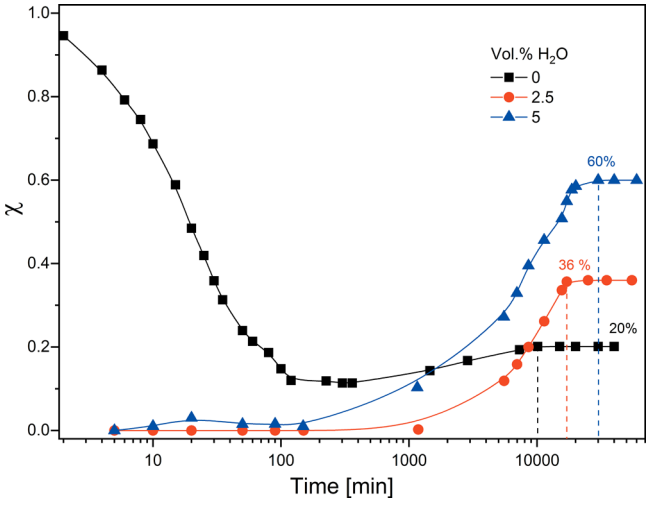

Figure 5. Molar fraction of $[Cm(nPr\ BTP)_3(NO_3)]^{2+}$ in 2 propanol with 0, 2.5, and 5 vol % H_2O as a function of time after the addition of nitrate. Dotted lines mark the attainment of the chemical equilibrium. $[Cm(III)]_{ini} = 1 \times 10^{-7}$ mol/L; [TBAN] = 4.03×10^{-5} mol/L.

Three important results are evident from Figure 5:

1. A higher water content results in the formation of a larger fraction of $[Cm(nPr\ BTP)_3(NO_3)]^{2+}$ (20% at 0 water, 36% at 2.5% water, 60% at 5% water). This is counterintuitive; higher water content is expected to stabilize the nitrate anion in solution, resulting in the formation of less $[Cm(nPr\ BTP)_3(NO_3)]^{2+}$.
2. The presence of water retards the formation of $[Cm(nPr\ BTP)_3(NO_3)]^{2+}$ and the time to reach the equilibrium doubles (0% H_2O, 5 days; 5% H_2O, 12 days).
3. $[Cm(nPr\ BTP)_3(NO_3)]^{2+}$ forms along a different reaction mechanism in pure 2 propanol, with a large fraction of $[Cm(nPr\ BTP)_3(NO_3)]^{2+}$ initially being formed as an intermediate product.

Effect of Nitrate Concentration. Experiments were performed at varied nitrate concentration to verify the formation of $[Cm(nPr\ BTP)_3(NO_3)]^{2+}$ in solution. The nitrate concentration was increased by adding TBAN while keeping the nPr BTP concentration constant. The samples were equilibrated for 5, 11, or 12 days depending on the solvent before performing TRLFS measurements. The normalized Cm(III) emission spectra in 2 propanol containing 2.5 vol % H_2O are shown in Figure 6. Cm(III) spectra in pure 2 propanol and 2 propanol containing 5 vol % H_2O are shown in the SI, Figure S3.

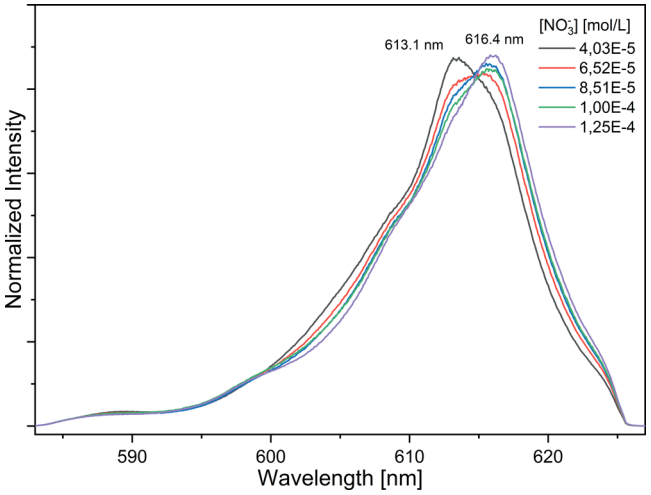

Figure 6. Normalized Cm(III) emission spectra as a function of the nitrate concentration. $[Cm(III)]_{ini} = 1 \times 10^{-7}$ mol/L, [nPr BTP] = 1.58×10^{-5} mol/L in 2 propanol containing 2.5 vol % H_2O.

The Cm(III) emission spectrum at 4.03×10^{-5} mol/L nitrate has an emission band at 613.1 nm and a shoulder at 616.4 nm. Increasing the nitrate concentration leads to a bathochromic shift of the Cm(III) emission band, indicating the formation of $[Cm(nPr\ BTP)_3(NO_3)]^{2+}$. The same trend was observed in pure 2 propanol and in 2 propanol containing 5 vol % H_2O.

Assuming the formation of the tenfold coordinated species according to eq 1,

$$[Cm(nPr\text{-}BTP)_3]^{3+} + NO_3^- \rightleftharpoons [Cm(nPr\text{-}BTP)_3(NO_3)]^{2+} \quad (1)$$

a plot of $\log(c([Cm(nPr\ BTP)_3(NO_3)]^{2+})/c([Cm(nPr\ BTP)_3]^{3+}))$ versus $\log([NO_3^-])$ should yield a slope of one. Results are shown in the SI, Figure S4, and Table 2. The slopes are close to 1. Slight deviations from the slope of 1 result from the limited number of data points due to the long

Table 2. Slopes and Conditional Stability Constants for the Formation of $[Cm(nPr\ BTP)_3(NO_3)]^{2+}$ in 2 Propanol and 2 Propanol with 2.5 and 5 vol % H_2O

vol % H_2O	0	2.5	5
Slope	1.00 ± 0.04	1.20 ± 0.08	1.12 ± 0.07
log K'	3.88 ± 0.13	4.22 ± 0.15	4.72 ± 0.12

times required to reach the chemical equilibrium. Yet, they clearly confirm the formation of the tenfold coordinated species $[Cm(nPr\ BTP)_3(NO_3)]^{2+}$.

Figure 7 shows the speciation of $[Cm(nPr\ BTP)_3(NO_3)]^{2+}$ and $[Cm(nPr\ BTP)_3]^{3+}$ in 2 propanol containing 2.5 vol % H_2O as a function of the nitrate concentration. The stability constant for the formation of the $[Cm(nPr\ BTP)_3(NO_3)]^{2+}$ complex according to eq 1 is log K' = 4.2 (see lines in Figure 7). The speciation diagrams for 2 propanol and 2 propanol with 5 vol % H_2O are shown in the SI, Figure S5. Stability constants are summarized in Table 2. They increase with increasing water content, which agrees with the trend shown in Figure 5.

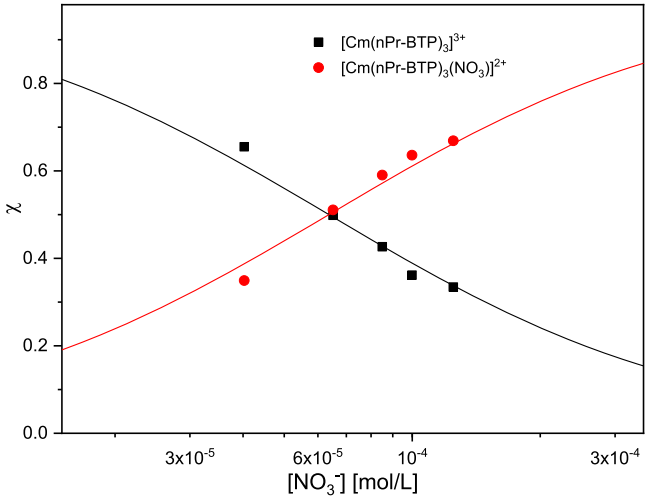

Figure 7. Molar fractions of $[Cm(nPr\ BTP)_3]^{3+}$ and $[Cm(nPr\ BTP)_3(NO_3)]^{2+}$ in 2 propanol containing 2.5 vol % H_2O as a function of the nitrate concentration. Lines calculated with log K' = 4.2.

Effect of nPr-BTP Concentration. To study the influence of the nPr BTP concentration on the formation of $[Cm(nPr\ BTP)_3(NO_3)]^{2+}$, complexation studies at constant nitrate concentration and increasing nPr BTP concentration in 2 propanol were performed.

Normalized Cm(III) fluorescence spectra in dependence of the nPr BTP concentration at constant nitrate concentration are shown in Figure 8.

Prior to the addition of nPr BTP only the solvated metal ion $[Cm(solv.)_9]^{3+}$ was observed, displaying a broad emission band at 600.5 nm corresponding to Cm(III) mainly coordinated by 2 propanol molecules.[58] Upon addition of 2×10^{-6} mol/L nPr BTP, $[Cm(nPr\ BTP)_3(NO_3)]^{2+}$ with its emission band at 617.3 nm formed exclusively. Further addition of nPr BTP reduced the fraction of this species in favor of the $[Cm(nPr\ BTP)_3]^{3+}$ complex with an emission maximum at 613.1 nm. The results show that the nitrate ion is not stabilized in the organic solvent at low nPr BTP concentrations, driving the formation of the $[Cm(nPr\ BTP)_3(NO_3)]^{2+}$ complex. At higher concentrations nPr BTP seems to be able to interact with the nitrate anion, stabilizing it in solution and thus promoting the formation of the $[Cm(nPr\ BTP)_3]^{3+}$ complex.

Effect of Anions, NO_2^-, CN^-, and OTf^-. Additional experiments at constant nitrite (NO_2^-), cyanide (CN^-), and triflate (OTf^-) concentrations and varying nPr BTP concentration were performed to investigate whether a tenfold

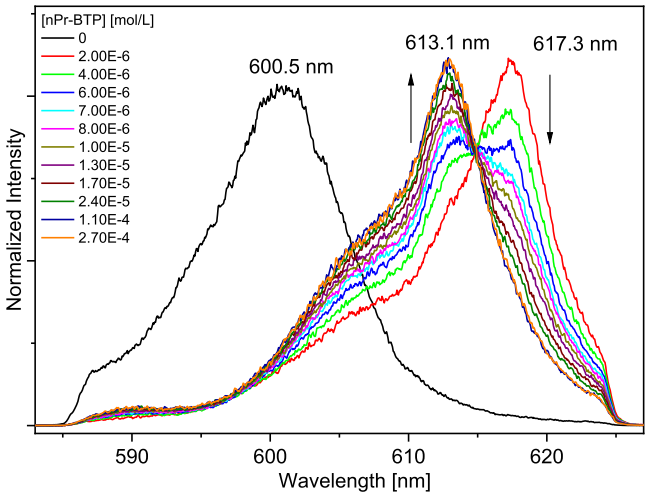

Figure 8. Normalized Cm(III) emission spectra as a function of the nPr BTP concentration in 2 propanol and a constant nitrate concentration. $[Cm(III)]_{ini} = 2 \times 10^{-7}$ mol/L; $[NO_3^-] = 2 \times 10^{-5}$ mol/L.

coordinated Cm(III) species may form with other small and hard anions, too. Similar to nitrate, these anions are generally weak or moderately strong ligands in aqueous solution but become strongly coordinating ligands in organic solutions. Because of the applied salts' poor solubility in 2 propanol the titration experiments were carried out in methanol and ethanol, respectively.

The normalized Cm(III) fluorescence spectra in dependence of the nPr BTP concentration at constant nitrite concentration are shown in Figure 9 (see SI, Figure S6 for cyanide and triflate).

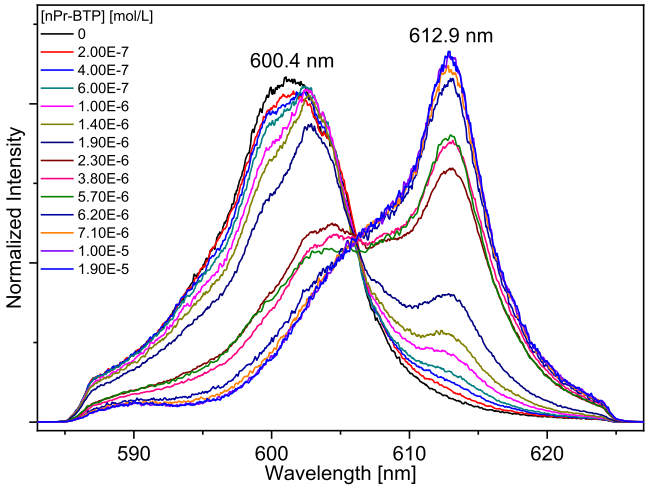

Figure 9. Normalized Cm(III) emission spectra as a function of the nPr BTP concentration in ethanol at constant nitrite concentration. $[Cm(III)]_{ini} = 2 \times 10^{-7}$ mol/L; $[NO_2^-] = 2 \times 10^{-5}$ mol/L.

Upon stepwise addition of nPr BTP, the solvated metal ion $[Cm(solv.)_9]^{3+}$ with an emission band at 600.4 nm (nitrite), 600.1 nm (cyanide), and 600.2 nm (triflate), respectively, transformed to the $[Cm(nPr\ BTP)_3]^{3+}$ complex with emission bands at 612.9 nm (nitrite, triflate) and 613.3 nm (cyanide), respectively. No further changes of the Cm(III) emission spectra were observed for nPr BTP concentrations greater than

1×10^{-5} mol/L (nitrite), 4×10^{-5} mol/L (cyanide), and 5×10^{-6} mol/L (triflate), respectively. An emission band pointing to the formation of a tenfold coordinated Cm(III) species was not observed; the tenfold coordinated Cm(III) species forms exclusively in the presence of nitrate.

The observation that no Cm(III) species with tenfold coordination forms with nitrite, cyanide, and triflate could be related to their size, solubility, or complexation strength in alcoholic solutions relative to nitrate.

Stability constants for the complexation of Cm(III) with nitrate, nitrite, cyanide, and triflate in alcoholic solution are not available. Stability constants for the complexation of Cm(III) with nitrate ($\log \beta^\circ_1 = 1.29$)[59] and Am(III) with both nitrate ($\log \beta^\circ_1 = 1.33$)[63] and nitrite ($\log \beta^\circ_1 = 2.10$)[63] do not explain the exclusive formation of a tenfold coordinated species with nitrate. Triflate is excluded due to its size and its weak complexation strength.

Solubility data of nitrate, nitrite, cyanide, and triflate salts in 2 propanol are not available. However, solubility data of NaCN, $NaNO_2$, and $NaNO_3$ in methanol and ethanol are available,[64] showing a significantly lower solubility of $NaNO_3$ compared to NaCN and $NaNO_2$ (see Table 3). This may explain the formation of the $[Cm(nPr\ BTP)_3X]^{2+}$ complex only with X = nitrate.

Table 3. Solubilities of Sodium Salts in Methanol and Ethanol[64]

	Solubility		
Salt	Methanol	Ethanol	Temperature
NaCN	6.05 wt %		15 °C
$NaNO_2$	4.24 wt %	0.31 wt %	19.5 °C
$NaNO_3$	0.41 wt %	0.036 wt %	25 °C

Structural Characterization of $[Cm(nPr\text{-}BTP)_3(NO_3)]^{2+}$—fluorescence Lifetimes. Having determined the stoichiometry of the $[Cm(nPr\ BTP)_3(NO_3)]^{2+}$ complex in solution, further studies were performed to elucidate its structure. Fluorescence lifetime measurements were performed at increasing nitrate concentration. The fluorescence lifetimes are summarized in Table 4. An example of the decrease of the fluorescence intensity as a function of the delay time is given in the SI, Figure S7.

The fluorescence lifetime of $[Cm(nPr\ BTP)_3]^{3+}$ in 2 propanol is $\tau = (361 \pm 18)\ \mu s$, which is in excellent agreement with literature data.[11,57] This is shorter than the theoretical lifetime of Cm(III) species in the absence of quenching ligands.[42] This is caused by nPr BTP quenching the Cm(III) fluorescence due to its aromatic system.[11,57]

Table 4. Fluorescence Lifetimes [μs] of Cm(III) with 1.58×10^{-5} mol/L nPr BTP at Different Nitrate Concentrations in 2 Propanol Containing 0, 2.5, and 5 vol % H_2O[a]

	vol % H_2O		
$[NO_3^-]$ [mol/L]	0	2.5	5
0	361		
4.03×10^{-5}	357	334	337
6.52×10^{-5}	351	326	
8.51×10^{-5}	347	338	
1.00×10^{-4}	345	330	330
1.25×10^{-4}	340	332	
1.49×10^{-4}			331

[a]Uncertainties are ±5%.

The fluorescence lifetime of $[Cm(nPr\ BTP)_3(NO_3)]^{2+}$ (which is the major species for nitrate concentrations > 10^{-4} mol/L; see Figure 7 and Table 2) is similar to that of $[Cm(nPr\ BTP)_3]^{3+}$. Since the fluorescence lifetime is dependent on the distance between the metal ion and the coordinating ligands, one can conclude that $[Cm(nPr\ BTP)_3]^{3+}$ and $[Cm(nPr\ BTP)_3(NO_3)]^{2+}$ have similar Cm(III)−N bond lengths.

Structural Characterization of $[Cm(nPr\text{-}BTP)_3(NO_3)]^{2+}$—VSBS. The structure of $[Cm(nPr\ BTP)_3(NO_3)]^{2+}$ was further investigated by VSBS.[65−68] The excitation of the probed metal ion results in internal vibrations which change the dipole moment of the ligand field, resulting in vibronic side bands (VSB). Accordingly, only vibrations of ligands directly coordinated to the central ion are observed in the VSB spectra. The experimental spectra consist of the zero phonon line (ZPL) resulting from the $^6D'_{7/2} \rightarrow {}^8S'_{7/2}$ transition as well as corresponding VSB. The wavelength range studied in detail is highlighted in Figure 10 (top). The energy of the different

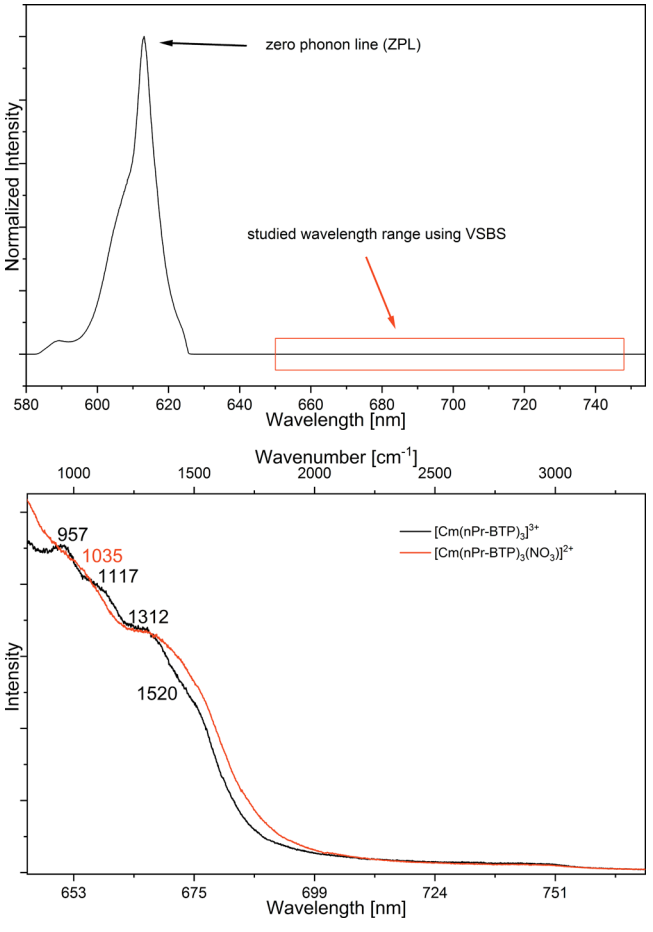

Figure 10. Top: Normalized Cm(III) emission spectrum representing the zero phonon line (ZPL) and the range studied using VSBS. Bottom: VSB spectrum of $[Cm(nPr\ BTP)_3]^{3+}$ in 2 propanol ($[Cm(III)]_{ini} = 1 \times 10^{-7}$ mol/L; [nPr BTP] = 2.23×10^{-5} mol/L) and VSB spectrum of a Cm(III) sample containing 64% $[Cm(nPr\ BTP)_3(NO_3)]^{2+}$ in 2 propanol with 2.5 vol % H_2O ($[Cm(III)]_{ini} = 1 \times 10^{-7}$ mol/L; [TBAN] = 1×10^{-4} mol/L; [nPr BTP] = 1.6×10^{-5} mol/L).

vibrations is the difference between the energy of the ZPL and the side bands according to eq 2.

$$E_{\text{vibration}} = E_{\text{ZPL}} - E_{\text{VSB}} \quad (2)$$

If a coordinated nitrate ion is present in the first coordination sphere of Cm(III), the NO stretching vibration should be visible in the side band spectrum of $[Cm(nPr\ BTP)_3(NO_3)]^{2+}$ when compared to the spectrum of the $[Cm(nPr\ BTP)_3]^{3+}$ complex. Figure 10 (bottom) shows the VSB spectra of $[Cm(nPr\ BTP)_3]^{3+}$ in 2 propanol and of a sample containing 64% of $[Cm(nPr\ BTP)_3(NO_3)]^{2+}$ in 2 propanol with 2.5 vol % H_2O. The derivative of both VSB spectra is given in the SI, Figure S8.

The zero phonon lines are located at $ZPL_{[Cm(nPr\text{-}BTP)3]3+}$ = 613.0 nm and $ZPL_{[Cm(nPr\text{-}BTP)3(NO3)]2+}$ = 616.3 nm. The VSB spectrum of $[Cm(nPr\ BTP)_3]^{3+}$ shows side bands at 957 cm^{-1}, 1117 cm^{-1}, 1312 cm^{-1}, and 1520 cm^{-1}. It differs from the VSB spectrum of the sample containing 64% $[Cm(nPr\ BTP)_3(NO_3)]^{2+}$, showing a distinct band at 1035 cm^{-1} which is not present in the VSB spectrum of $[Cm(nPr\ BTP)_3]^{3+}$ and is assigned to a nitrate stretching mode.

Computational Results. To assign the experimental VSB, DFT calculations investigating potential positions of the nitrate in the complex are mandatory. Therefore, various structures of the tenfold coordinated species were optimized and VSB spectra were calculated. Calculations were performed with 2,6 bis(5,6 dimethyl 1,2,4 triazin 3 yl)pyridine (Me BTP) instead of nPr BTP due to the similar steric demand and the reduced computational effort.

Four energy minima were found, with the nitrate located on either of the two symmetry axes (C_2 and C_3) of the D_3 symmetrical complex (see Figure 11). The nitrate is positioned either at a short Cm−ONO_2 distance (Figure 11, positions a,c) or a long Cm−ONO_2 distance (Figure 11, positions b, d) on one of the two symmetry axes.

Gas phase energies E_0 were calculated according to eq 3 for complexes a−d and three different solvent clusters L = $(H_2O)_8$, (2 propanol)$_4$$(H_2O)_4$, and (2 propanol)$_8$. For all complexation reactions negative reaction enthalpies were computed (except for position a and 8 iPrOH). Calculated relative reaction energies are given in Table 5.

$$[Cm(Me\text{-}BTP)_3]^{3+} + NO_3^-\cdot L \rightleftharpoons [Cm(Me\text{-}BTP)_3(NO_3)]^{2+} + L \quad (3)$$

The lowest reaction energy was determined for the nitrate in position (b) in water, slightly lower than for position (c) in water. However, based on the quantum chemical calculations alone, we cannot definitely discard either position (b) or (c) as present in solution. Reaction energies were found to increase with the number of 2 propanol molecules. This trend is in excellent agreement with the stability constants log K' increasing with the water content (cf. Table 2). Regardless of the solvent cluster, the lowest energy was always observed for (b).

The optimized structure of the energetically most favored $[Cm(Me\ BTP)_3(NO_3)]^{2+}$ complex with the nitrate in position (b) is shown in Figure 12 with a Cm−ONO_2 distance of $r_{Cm\text{-}O}$ = 413 pm. The other $[Cm(Me\ BTP)_3(NO_3)]^{2+}$ structures are shown in the SI, Figure S9.

Bond lengths of $r_{Cm\text{-}O}$ = 246 pm and $r_{Cm\text{-}O}$ = 233 pm are determined for the positions (a) and (c), respectively. The bond length for (d) is $r_{Cm\text{-}O}$ is 558 pm. This is longer by 145 pm compared to (b). This structure is hence both

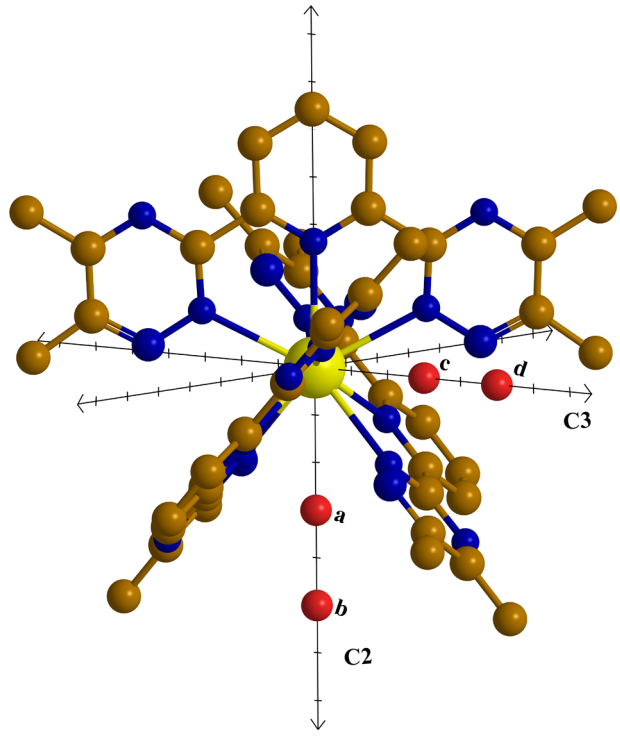

Figure 11. Scheme of the different positions of the nitrate on the symmetry axes of $[Cm(Me\ BTP)_3]^{3+}$ resulting in energy minima. Carbon (brown), nitrogen (blue), curium (yellow), nitrate (red).

Table 5. Energy Differences of the $[Cm(Me\ BTP)_3(NO_3)]^{2+}$ Complexes in Different Solvents Relative to the Most Stable One ($\Delta E_{\text{position b, H2O}}$), Calculated at the B3 LYP/def2 TZVP Level of Theory

L	$\Delta E_{\text{position\_a}}$ [kJ/mol]	$\Delta E_{\text{position\_b}}$ [kJ/mol]	$\Delta E_{\text{position\_c}}$ [kJ/mol]	$\Delta E_{\text{position\_d}}$ [kJ/mol]
8 H_2O	62.4	0	0.3	21.4
4 H_2O + 4 iPrOH	75.5	13.1	13.3	34.5
8 iPrOH	105.4	43.0	43.2	64.4

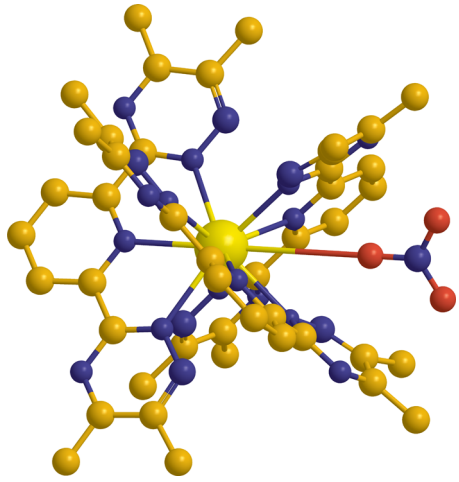

Figure 12. Optimized structure of $[Cm(Me\ BTP)_3(NO_3)]^{2+}$ with nitrate in position (b). Hydrogen atoms are omitted for clarity. Carbon (brown), nitrogen (blue), oxygen (red), curium (yellow).

energetically (Table 5) and structurally discarded: coordination of nitrate with such a long distance would not cause a significant red shift of the fluorescence band.

To evaluate the experimental VSB spectra shown in Figure 10 (bottom), VSB spectra for the optimized structures of $[Cm(Me\ BTP)_3]^{3+}$ and $[Cm(Me\ BTP)_3(NO_3)]^{2+}$ were calculated. They are shown in Figure 13.

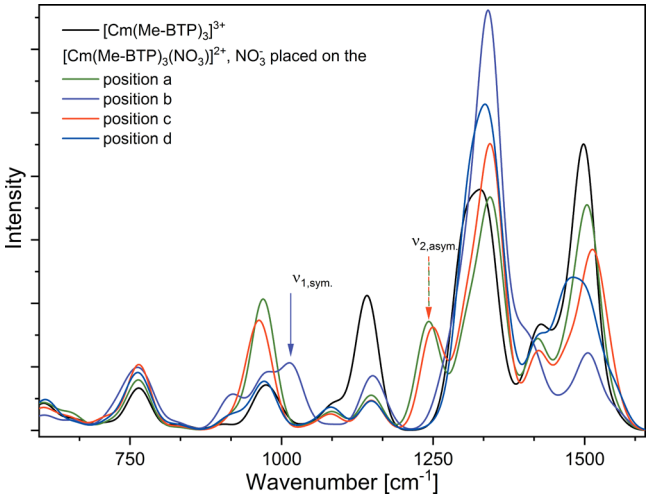

Figure 13. Calculated VSB spectra of the $[Cm(Me\ BTP)_3]^{3+}$ and the $[Cm(Me\ BTP)_3(NO_3)]^{2+}$ complexes with the nitrate in positions a–d.

All calculated VSB spectra show vibrational modes at 969 cm^{-1}, 1145 cm^{-1}, 1337 cm^{-1}, and 1500 cm^{-1}. These are attributed to vibrations of the BTP framework (cf. SI, Figure S10). The calculated energies of the vibrational modes of the nitrate and their assignments are given in Table 6. An illustration of the vibrational modes of the nitrate is shown in the SI, Figure S11.

Table 6. Assignment and Energy of the Vibrational Modes of the Coordinated Nitrate for the Different Calculated Structures of $[Cm(Me\ BTP)_3(NO_3)]^{2+}$[a]

	E_{vib} [cm^{-1}]					
NO_3^- position	δ_1	δ_2	$\delta_{3,\ out\ of\ plane}$	$\nu_{1,sym.}$	$\nu_{2,asym.}$	ν_3
a	668	718	792	994	**1277**	1547
b	680	688	802	**1047**	1311	1556
c	663	724	790	981	**1285**	1574
d	705	702	805	1061	1361	

[a]Vibrational modes not covered by vibrational modes from the BTP framework are highlighted.

Bending modes δ_n of the nitrate are in the range of 663–805 cm^{-1} while stretching modes ν_n are in the range of 981–1574 cm^{-1}. Unfortunately, most of the vibrational modes resulting from the nitrate are superimposed by BTP framework vibrations. However, $\nu_{1,sym.}$ of $[Cm(Me\ BTP)_3(NO_3)]^{2+}$ in which the nitrate is positioned on (b) (energetically most favorable structure) and $\nu_{2,asym.}$ of $[Cm(Me\ BTP)_3(NO_3)]^{2+}$ with the nitrate in position (a) or (c) are not covered by vibrational modes of the BTP framework. These vibrations are highlighted in Table 6 and Figure 13. They are used for comparison with the experimental VSB spectra.

Comparison of Calculated and Experimental VSB Spectra. Calculated VSB of the energetically most favored $[Cm(Me\ BTP)_3(NO_3)]^{2+}$ complexes with the nitrate positioned on (b) and (c) and of $[Cm(nPr\ BTP)_3]^{3+}$ are compared to the experimental data; see Figure 14. The only observable

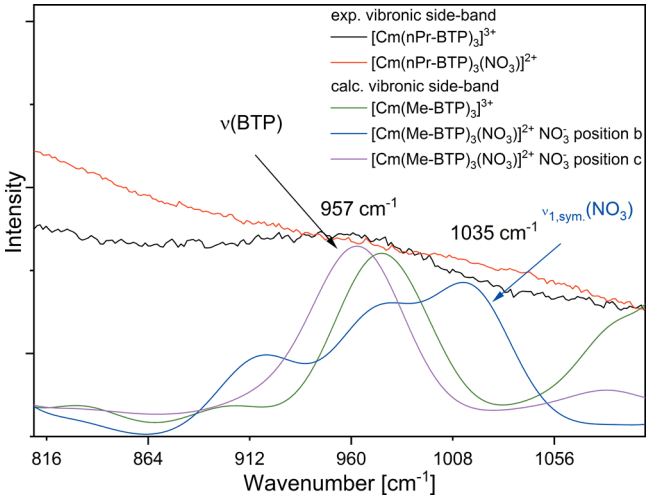

Figure 14. Comparison of experimental VSB spectra of $[Cm(nPr\ BTP)_3]^{3+}$ and $[Cm(nPr\ BTP)_3(NO_3)]^{2+}$ (64%) and calculated VSB spectra of $[Cm(Me\ BTP)_3]^{3+}$ and $[Cm(Me\ BTP)_3(NO_3)]^{2+}$ (with the nitrate in position (b) or (c)).

difference between the experimental VSB spectra of $[Cm(nPr\ BTP)_3(NO_3)]^{2+}$ and $[Cm(nPr\ BTP)_3]^{3+}$ is the side band at 1035 cm^{-1} (cf. Figure 10 bottom). Comparison with the calculated VSB spectra focuses on this wavelength region.

The VSB at 957 cm^{-1} is observed experimentally both in the sample containing 64% $[Cm(nPr\ BTP)_3(NO_3)]^{2+}$ and in the $[Cm(nPr\ BTP)_3]^{3+}$ sample. It is well reproduced in the calculated VSB of $[Cm(Me\ BTP)_3(NO_3)]^{2+}$ and $[Cm(Me\ BTP)_3]^{3+}$. This VSB is assigned to a vibrational mode of the BTP framework.

However, the VSB at 1035 cm^{-1} observed experimentally in the sample containing 64% $[Cm(nPr\ BTP)_3(NO_3)]^{2+}$ is only reproduced in the calculated VSB spectrum of $[Cm(Me\ BTP)_3(NO_3)]^{2+}$ with the nitrate in position (b). This VSB is attributed to the symmetric nitrate stretching mode $\nu_{1,sym}$.

Combining DFT calculations and results from VSBS allows assigning the position of the nitrate in the $[Cm(nPr\ BTP)_3(NO_3)]^{2+}$ species: it is located on the C_2 axis with a Cm ONO_2 distance of $r_{Cm\text{-}O}$ = 413 pm.

XPS Measurements. The tenfold coordination of trivalent actinides was further investigated by X ray photoelectron spectroscopy (XPS).

First, the N 1s and C 1s photoelectron spectra of nPr BTP in the presence and absence of HNO_3 were recorded. BTP are known to form nPr BTP·$n$$HNO_3$ (n = 1,2) adducts.[1,69] The spectra are shown in the SI, Figure S12. The N 1s main lines and the C 1s spectra show only subtle differences in the presence or absence of HNO_3. However, an additional peak at 406.8 eV in the N 1s spectrum of nPr BTP containing HNO_3 is observed, indicating adduct formation. The peak area ratio of the N 1s BTP signal and the N 1s nitrate signal (after subtraction of a Shirley background) is 7:1, corroborating the

formation of nPr BTP·HNO_3 (seven N from BTP, one N from HNO_3).

Then, the $[M(nPr\ BTP)_3(NO_3)]^{2+}$ complexes (M = Am, Eu) (analogue for Cm(III)) were synthesized and photo electron spectra were measured. The Am 4f spectrum is shown in Figure S13. The N 1s and C 1s photoelectron spectra are shown in Figure 15 together with the photoelectron spectrum of nPr BTP.

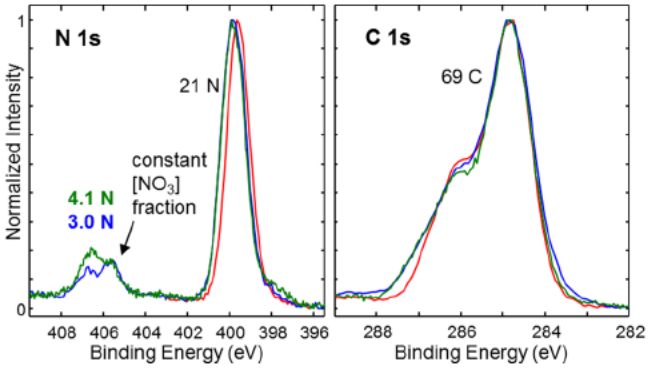

Figure 15. Comparison of the photoelectron spectra of nPr BTP (red curve) and the $[M(nPr\ BTP)_3(NO_3)]^{2+}$ complexes (M = Eu, blue curve and Am, green curve) in 2 propanol (nPr BTP and Eu(III) complex) or 2 propanol with 0.15 mol/L HNO_3 (Am(III) complex). $[Eu(NO_3)_3] = [Am(NO_3)_3] = 1 \times 10^{-3}$ mol/L; [nPr BTP] = 3×10^{-3} mol/L.

Compared to the photoelectron spectrum of nPr BTP, both the aromatic region of the C 1s spectrum and the N 1s spectrum of the Am(III) and Eu(III) complexes show slight shifts toward higher binding energies. This indicates a decreased electron density in the aromatic system due to complexation of Am(III) and Eu(III). Comparing the photoelectron spectra of the Am(III) and Eu(III) complexes, no significant differences are observed.

The Am(III) and Eu(III) complexes show two peaks in the nitrate region of the N 1s spectrum: 405.6 eV ($nitrate_1$) and 406.7 eV ($nitrate_2$). The $M(nPr\ BTP)_3$:$nitrate_1$:$nitrate_2$ peak area ratios after subtraction of a Shirley background are 21:2:1 for Eu(III) and 21:2:2 for Am(III).

Indeed, two nitrate peaks with a 2:1 ratio are expected in a $[M(nPr\ BTP)_3(NO_3)](NO_3)_2$ species. The XPS results of the Eu(III) complex are in excellent agreement. In contrast to the Eu(III) stock solution, the Am(III) stock solution contained nitric acid. Thus, the 2:2 ratio in the nitrate region of the Am(III) species could be due to adduct formation, $[Am(nPr\ BTP)_3(NO_3)](NO_3)_2 \cdot HNO_3$,[1,69] with superimposed $nitrate_2$ and $nitrate_{adduct}$ peaks.

The adduct formation was further investigated by preparing the $[Eu(nPr\ BTP)_3(NO_3)](NO_3)_2$ complex in the presence of increasing amounts of HNO_3. The corresponding N 1s and C 1s photoelectron spectra are shown in Figure 16. The peak at 406.7 eV in the nitrate region of the N 1s spectrum grows in intensity with increasing nitric acid concentration. According to the peak areas, the related species are $[Eu(nPr\ BTP)_3(NO_3)](NO_3)_2 \cdot 2HNO_3$ and $[Eu(nPr\ BTP)_3(NO_3)](NO_3)_2 \cdot 3HNO_3$.

Thus, the N 1s elemental line of nitrate at 406.7 eV is assigned to one nitrate bound directly to the trivalent metal ion and to adduct HNO_3 molecules. The nitrate signals at 405.6 eV correspond to two outer sphere nitrate anions. XPS

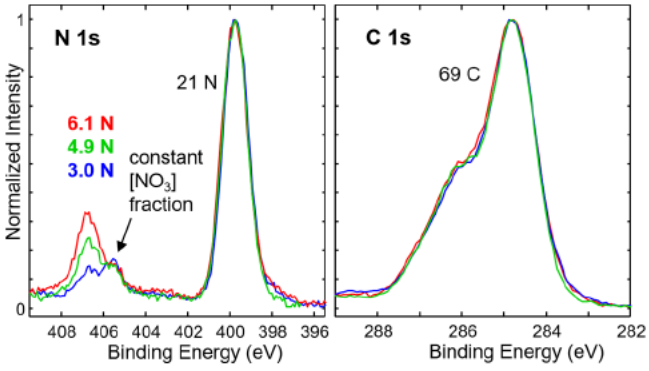

Figure 16. Photoelectron spectra of $[Eu(nPr\ BTP)_3(NO_3)](NO_3)_2 \cdot xHNO_3$ complexes in 2 propanol with 0 (blue curve), 0.18 (green curve), and 0.5 mol/L HNO_3 (red curve). $[Eu(NO_3)_3] = 1 \times 10^{-3}$ mol/L; [nPr BTP] = 3×10^{-3} mol/L.

measurements, therefore, verify the formation of $[Am(nPr\ BTP)_3(NO_3)]^{2+}$ and $[Eu(nPr\ BTP)_3(NO_3)]^{2+}$ species.

CONCLUSION

The complexation of Am(III), Cm(III), and Eu(III) with nPr BTP in the presence of nitrate dissolved in 2 propanol was studied by TRLFS, VSBS, DFT, and XPS. The combined results unambiguously confirm the formation of a tenfold coordinated Cm(III) complex, $[Cm(nPr\ BTP)_3(NO_3)]^{2+}$ in solution.

With TRLFS a bathochromic shift of 4.1 nm with respect to the emission spectrum from $[Cm(nPr\ BTP)_3]^{3+}$ was observed. This was assigned to the additional coordination of a nitrate anion, forming $[Cm(nPr\ BTP)_3(NO_3)]^{2+}$ in solution. The formation of this species, verified by slope analyses, exhibits slow kinetics in the range of 5−12 days, depending on the water content of the solvent. Contrary to expectations, an increased water content in the solvent promotes its formation. Also, $[Cm(nPr\ BTP)_3(NO_3)]^{2+}$ is only found at low nPr BTP concentrations. The presence of high nPr BTP concentrations favors the ninefold coordinated complex, indicating that the free ligand molecules stabilize the nitrate in solution.

VSBS provided additional evidence for the presence of a coordinated nitrate anion. In combination with DFT calculations, the coordinated nitrate was shown to be located on the C_2 axis of the D_3 symmetrical ninefold coordinated complex with a Cm−ONO_2 distance of $r_{Cm\text{-}O}$ = 413 pm.

Further evidence for the existence of $[M(nPr\ BTP)_3(NO_3)]^{2+}$ complexes with tenfold coordination was provided by XPS measurements of the corresponding Am(III) and Eu(III) complexes. N 1s photoelectron spectra reveal two distinct nitrate signals resulting from inner sphere and outer sphere nitrate ions.

The literature shows trivalent actinides to be ninefold coordinated in aqueous solutions. This study marks the first evidence of a trivalent actinide complex with tenfold coordination in solution. In contrast to most other studies, this study was performed in nonaqueous solution, which may explain the unique stability of the tenfold coordinated complex.

ASSOCIATED CONTENT

Supporting Information

The Supporting Information is available free of charge at https://pubs.acs.org/doi/10.1021/acs.inorgchem.0c01526.

Cm(III) emission spectra as a function of time or nitrate concentration for the systems containing 0, 2.5, and 5 vol % H_2O; example of a peak deconvolution; slope analyses and speciation diagrams;. Cm(III) emission spectra as a function of CN^- and OTf^-; optimized structures of $[Cm(Me\ BTP)_3(NO_3)]^{2+}$; and further XPS data (PDF)

AUTHOR INFORMATION

Corresponding Author

Patrik Weßling − *Karlsruhe Institute of Technology (KIT), Institute for Nuclear Waste Disposal (INE), 76021 Karlsruhe, Germany; Ruprecht Karls Universität Heidelberg, Institut für Physikalische Chemie, 69120 Heidelberg, Germany;* orcid.org/0000 0002 4410 5344; Phone: +4972160824652; Email: patrik.wessling@kit.edu

Authors

Tobias Schenk − *Ruprecht Karls Universität Heidelberg, Institut für Physikalische Chemie, 69120 Heidelberg, Germany*

Felix Braun − *Ruprecht Karls Universität Heidelberg, Institut für Physikalische Chemie, 69120 Heidelberg, Germany*

Björn B. Beele − *Bergische Universität Wuppertal, Inorganic Chemistry, 42119 Wuppertal, Germany;* orcid.org/0000 0001 5888 8952

Sascha Trumm − *Karlsruhe Institute of Technology (KIT), Center for Advanced Technological and Environmental Training (FTU), 76021 Karlsruhe, Germany*

Michael Trumm − *Karlsruhe Institute of Technology (KIT), Institute for Nuclear Waste Disposal (INE), 76021 Karlsruhe, Germany*

[⊥]Bernd Schimmelpfennig − *Karlsruhe Institute of Technology (KIT), Institute for Nuclear Waste Disposal (INE), 76021 Karlsruhe, Germany*

Dieter Schild − *Karlsruhe Institute of Technology (KIT), Institute for Nuclear Waste Disposal (INE), 76021 Karlsruhe, Germany;* orcid.org/0000 0001 6034 8146

Andreas Geist − *Karlsruhe Institute of Technology (KIT), Institute for Nuclear Waste Disposal (INE), 76021 Karlsruhe, Germany*

Petra J. Panak − *Karlsruhe Institute of Technology (KIT), Institute for Nuclear Waste Disposal (INE), 76021 Karlsruhe, Germany; Ruprecht Karls Universität Heidelberg, Institut für Physikalische Chemie, 69120 Heidelberg, Germany*

Author Contributions

All authors have given approval to the final version of the manuscript. All authors contributed equally.

Funding

This work has received funding from the European Research Council (ERC) under the European Union's Horizon 2020 research and innovation program (project GENIORS, grant agreement *N*° 755171).

Notes

The authors declare no competing financial interest.

[⊥]Deceased, 13 September 2019.

REFERENCES

(1) Kolarik, Z.; Müllich, U.; Gassner, F. Extraction of Am(III) and Eu(III) nitrates by 2,6 di (5,6 dipropyl 1,2,4 triazin 3 yl)pyridines. *Solvent Extr. Ion Exch.* **1999**, *17* (5), 1155−1170.

(2) Ekberg, C.; Fermvik, A.; Retegan, T.; Skarnemark, G.; Foreman, M. R. S.; Hudson, M. J.; Englund, S.; Nilsson, M. An overview and historical look back at the solvent extraction using nitrogen donor ligands to extract and separate An(III) from Ln(III). *Radiochim. Acta* **2008**, *96* (4−5), 225−233.

(3) Lewis, F. W.; Hudson, M. J.; Harwood, L. M. Development of highly selective ligands for separations of actinides from lanthanides in the nuclear fuel cycle. *Synlett* **2011**, *2011* (18), 2609−2632.

(4) Hudson, M. J.; Lewis, F. W.; Harwood, L. M., The circuitous journey from malonamides to BTPhens: ligands for separating actinides from lanthanides. In *Strategies and Tactics in Organic Synthesis*; Michael, H., Ed.; Academic Press: 2013; Vol. 9, pp 177−202.

(5) Panak, P. J.; Geist, A. Complexation and extraction of trivalent actinides and lanthanides by triazinylpyridine N donor ligands. *Chem. Rev.* **2013**, *113* (2), 1199−1236.

(6) Iveson, P. B.; Riviere, C.; Guillaneux, D.; Nierlich, M.; Thuery, P.; Ephritikhine, M.; Madic, C. Selective complexation of uranium (III) over cerium(III) by 2,6 bis(5,6 dialkyl 1,2,4 triazin 3 yl) pyridines: H 1 NMR and X ray crystallography studies. *Chem. Commun.* **2001**, No. 16, 1512−1513.

(7) Denecke, M. A.; Rossberg, A.; Panak, P. J.; Weigl, M.; Schimmelpfennig, B.; Geist, A. Characterization and comparison of Cm(III) and Eu(III) complexed with 2,6 di(5,6 dipropyl 1,2,4 triazin 3 yl)pyridine using EXAFS, TRFLS, and quantum chemical methods. *Inorg. Chem.* **2005**, *44* (23), 8418−8425.

(8) Denecke, M. A.; Panak, P. J.; Burdet, F.; Weigl, M.; Geist, A.; Klenze, R.; Mazzanti, M.; Gompper, K. A comparative spectroscopic study of U(III)/Am(III) and Ln(III) complexed with N donor ligands. *C. R. Chim.* **2007**, *10* (10−11), 872−882.

(9) Banik, N. L.; Schimmelpfennig, B.; Marquardt, C. M.; Brendebach, B.; Geist, A.; Denecke, M. A. Characterization of redox sensitive plutonium(III) complexed with alkylated 2,6 ditriazinylpyridine (BTP) in organic solution. *Dalton Trans.* **2010**, *39* (21), 5117−5122.

(10) Adam, C.; Kaden, P.; Beele, B. B.; Müllich, U.; Trumm, S.; Geist, A.; Panak, P. J.; Denecke, M. A. Evidence for covalence in a N donor complex of americium(III). *Dalton Trans.* **2013**, *42* (39), 14068−14074.

(11) Trumm, S.; Panak, P. J.; Geist, A.; Fanghänel, T. A TRLFS study on the complexation of Cm(III) and Eu(III) with 2,6 bis(5,6 dipropyl 1,2,4 triazin 3 yl)pyridine in water/methanol mixture. *Eur. J. Inorg. Chem.* **2010**, *2010* (19), 3022−3028.

(12) Berthet, J. C.; Miquel, Y.; Iveson, P. B.; Nierlich, M.; Thuery, P.; Madic, C.; Ephritikhine, M. The affinity and selectivity of terdentate nitrogen ligands towards trivalent lanthanide and uranium ions viewed from the crystal structures of the 1:3 complexes. *J. Chem. Soc., Dalton Trans.* **2002**, No. 16, 3265−3272.

(13) Drew, M. G. B.; Guillaneux, D.; Hudson, M. J.; Iveson, P. B.; Russell, M. L.; Madic, C. Lanthanide(III) complexes of a highly efficient actinide(III) extracting agent — 2,6 bis(5,6 dipropyl 1,2,4 triazin 3 yl)pyridine. *Inorg. Chem. Commun.* **2001**, *4* (1), 12−15.

(14) Colette, S.; Amekraz, B.; Madic, C.; Berthon, L.; Cote, G.; Moulin, C. Use of electrospray mass spectrometry (ESI MS) for the study of europium(III) complexation with bis(dialkyltriazinyl) pyridines and its implications in the design of new extracting agents. *Inorg. Chem.* **2002**, *41* (26), 7031−7041.

(15) Colette, S.; Amekraz, B.; Madic, C.; Berthon, L.; Cote, G.; Moulin, C. Europium(III) interaction with a polyaza aromatic extractant studied by time resolved laser induced luminescence: A thermodynamical approach. *Inorg. Chem.* **2004**, *43* (21), 6745−6751.

(16) Rawat, N.; Bhattacharyya, A.; Ghosh, S. K.; Gadly, T.; Tomar, B. S. Thermodynamics of complexation of lanthanides with 2,6 bis(5,6 diethyl 1,2,4 triazin 3 yl) pyridine. *Radiochim. Acta* **2011**, *99* (11), 705−712.

(17) Banik, N. L.; Denecke, M. A.; Geist, A.; Modolo, G.; Panak, P. J.; Rothe, J. 2,6 Bis(5,6 dipropyl 1,2,4 triazin 3 yl) pyridine: structures of An(III) and Ln(III) 1:3 complexes and selectivity. *Inorg. Chem. Commun.* **2013**, *29*, 172−174.
(18) Karraker, D. G. Hypersensitive transitions of hydrated neodymium(III), holmium(III) and erbium(III) ions. *Inorg. Chem.* **1968**, *7* (3), 473−479.
(19) Steele, M. L.; Wertz, D. L. Solute complexes in aqueous gadolinium(III) chloride solutions. *J. Am. Chem. Soc.* **1976**, *98* (15), 4424−4428.
(20) Habenschuss, A.; Spedding, F. H. The coordination (hydration) of rare earth ions in aqueous chloride solutions from x ray diffraction. I. $TbCl_3$,$DyCl_3$, $ErCl_3$,$TmCl_3$, and $LuCl_3$. *J. Chem. Phys.* **1979**, *70* (6), 2797−2806.
(21) Habenschuss, A.; Spedding, F. H. The coordination (hydration) of rare earth ions in aqueous chloride solutions from x ray diffraction. II. $LaCl_3$, $PrCl_3$, and $NdCl_3$. *J. Chem. Phys.* **1979**, *70* (8), 3758−3763.
(22) Habenschuss, A.; Spedding, F. H. The coordination (hydration) of rare earth ions in aqueous chloride solutions from x ray diffraction. III. $SmCl_3$, $EuCl_3$, and series behavior. *J. Chem. Phys.* **1980**, *73* (1), 442−450.
(23) Allen, P. G.; Bucher, J. J.; Shuh, D. K.; Edelstein, N. M.; Craig, I. Coordination chemistry of trivalent lanthanide and actinide ions in dilute and concentrated chloride solutions. *Inorg. Chem.* **2000**, *39* (3), 595−601.
(24) Persson, I.; D'Angelo, P.; De Panfilis, S.; Sandström, M.; Eriksson, L. Hydration of lanthanoid(III) ions in aqueous solution and crystalline hydrates studied by EXAFS spectroscopy and crystallography: the myth of the "gadolinium break". *Chem. Eur. J.* **2008**, *14* (10), 3056−3066.
(25) Lindqvist Reis, P.; Apostolidis, C.; Rebizant, J.; Morgenstern, A.; Klenze, R.; Walter, O.; Fanghänel, T.; Haire, R. G. The structures and optical spectra of hydrated transplutonium ions in the solid state and in solution. *Angew. Chem., Int. Ed.* **2007**, *46* (6), 919−922.
(26) Solera, J. A.; García, J.; Proietti, M. G. Multielectron excitations at the L edges in rare earth ionic aqueous solutions. *Phys. Rev. B: Condens. Matter Mater. Phys.* **1995**, *51* (5), 2678−2686.
(27) Hasegawa, Y.; Tsuruoka, S. I.; Yoshida, T.; Kawai, H.; Kawai, T. Emission properties of Sm(III) complex having ten coordination structure. *Thin Solid Films* **2008**, *516* (9), 2704−2707.
(28) Choppin, G. R. Comparative solution chemistry of the 4f and 5f elements. *J. Alloys Compd.* **1995**, *223* (2), 174−179.
(29) Allen, P. G.; Bucher, J. J.; Shuh, D. K.; Edelstein, N. M.; Reich, T. Investigation of aquo and chloro complexes of UO_2^{2+}, NpO_2^{+}, Np^{4+}, and Pu^{3+} by X ray absorption fine structure spectroscopy. *Inorg. Chem.* **1997**, *36* (21), 4676−4683.
(30) Runde, W.; Van Pelt, C.; Allen, P. G. Spectroscopic characterization of trivalent f element (Eu, Am) solid carbonates. *J. Alloys Compd.* **2000**, *303*−*304*, 182−190.
(31) Brendebach, B.; Banik, N. L.; Marquardt, C. M.; Rothe, J.; Denecke, M.; Geckeis, H. X ray absorption spectroscopic study of trivalent and tetravalent actinides in solution at varying pH values. *Radiochim. Acta* **2009**, *97* (12), 701−708.
(32) David, F. H.; Fourest, B. Structure of trivalent lanthanide and actinide aquo ions. *New J. Chem.* **1997**, *21* (2), 167−176.
(33) Antonio, R.; Soderholm, L.; Williams, C. W.; Blaudeau, J. P.; Bursten, B. E. Neptunium redox speciation. *Radiochim. Acta* **2001**, *89* (1), 17−25.
(34) Conradson, S. D. Application of X ray absorption fine structure spectroscopy to materials and environmental science. *Appl. Spectrosc.* **1998**, *52* (7), 252A−279A.
(35) Conradson, S. D.; Abney, K. D.; Begg, B. D.; Brady, E. D.; Clark, D. L.; den Auwer, C.; Ding, M.; Dorhout, P. K.; Espinosa Faller, F. J.; Gordon, P. L.; Haire, R. G.; Hess, N. J.; Hess, R. F.; Keogh, D. W.; Lander, G. H.; Lupinetti, A. J.; Morales, L. A.; Neu, M. P.; Palmer, P. D.; Paviet Hartmann, P.; Reilly, S. D.; Runde, W. H.; Tait, C. D.; Veirs, D. K.; Wastin, F. Higher order speciation effects on plutonium L3 X ray absorption near edge spectra. *Inorg. Chem.* **2004**, *43* (1), 116−131.
(36) Carnall, W. T. Crystal field analysis of $LaCl_3$:Am^{3+} and $AmCl_3$ and its relationship to the spectra of frozen solutions of Am^{3+} (aquo). *J. Less Common Met.* **1989**, *156* (1), 221−235.
(37) Kimura, T.; Kato, Y. Luminescence study on determination of the inner sphere hydration number of Am(III) and Nd(III). *J. Alloys Compd.* **1998**, *271*−*273*, 867−871.
(38) Adam, C.; Beele, B. B.; Geist, A.; Müllich, U.; Kaden, P.; Panak, P. J. NMR and TRLFS studies of Ln(III) and An(III) C5 BPP complexes. *Chem. Sci.* **2015**, *6* (2), 1548−1561.
(39) Adam, C.; Rohde, V.; Müllich, U.; Kaden, P.; Geist, A.; Panak, P. J.; Geckeis, H. Comparative NMR study of nPrBTP and iPrBTP. *Procedia Chem.* **2016**, *21*, 38−45.
(40) Lindqvist Reis, P.; Klenze, R.; Schubert, G.; Fanghänel, T. Hydration of Cm^{3+} in aqueous solution from 20 to 200 °C. A time resolved laser fluorescence spectroscopy study. *J. Phys. Chem. B* **2005**, *109* (7), 3077−3083.
(41) Kimura, T.; Choppin, G. R. Luminescence study on determination of the hydration number of Cm(III). *J. Alloys Compd.* **1994**, *213*, 313−317.
(42) Kimura, T.; Choppin, G. R.; Kato, Y.; Yoshida, Z. Determination of the hydration number of Cm(III) in various aqueous solutions. *Radiochim. Acta* **1996**, *72* (2), 61−64.
(43) Kimura, T.; Nagaishi, R.; Kato, Y.; Yoshida, Z. Luminescence study on solvation of americium(III), curium(III) and several lanthanide(III) ions in nonaqueous and binary mixed solvents. *Radiochim. Acta* **2001**, *89* (3), 125−130.
(44) Ikeda Ohno, A.; Hennig, C.; Rossberg, A.; Funke, H.; Scheinost, A. C.; Bernhard, G.; Yaita, T. Electrochemical and complexation behavior of neptunium in aqueous perchlorate and nitrate solutions. *Inorg. Chem.* **2008**, *47* (18), 8294−8305.
(45) Denecke, M. A. Actinide speciation using X ray absorption fine structure spectroscopy. *Coord. Chem. Rev.* **2006**, *250* (7−8), 730−754.
(46) Choppin, G. R.; Thakur, P.; Mathur, J. N. Complexation thermodynamics and structural aspects of actinide−aminopolycarboxylates. *Coord. Chem. Rev.* **2006**, *250* (7−8), 936−947.
(47) Case, F. H. Preparation of 2,4 bis triazinyl and 2,6 bis triazinyl and triazolinyl derivatives of pyridine. *J. Heterocycl. Chem.* **1971**, *8* (6), 1043−1046.
(48) Seah, M. P.; Gilmore, I. S.; Beamson, G. XPS: binding energy calibration of electron spectrometers 5—re evaluation of the reference energies. *Surf. Interface Anal.* **1998**, *26* (9), 642−649.
(49) *TURBOMOLE* V7.0; TURBOMOLE GmbH, www.turbomole.com. 1989−2007.
(50) Perdew, J. P. Density functional approximation for the correlation energy of the inhomogeneous electron gas. *Phys. Rev. B: Condens. Matter Mater. Phys.* **1986**, *33* (12), 8822−8824.
(51) Becke, A. D. Density functional exchange energy approximation with correct asymptotic behavior. *Phys. Rev. A: At., Mol., Opt. Phys.* **1988**, *38* (6), 3098−3100.
(52) Eichkorn, K.; Weigend, F.; Treutler, O.; Ahlrichs, R. Auxiliary basis sets for main row atoms and transition metals and their use to approximate Coulomb potentials. *Theor. Chem. Acc.* **1997**, *97* (1), 119−124.
(53) Küchle, W.; Dolg, M.; Stoll, H.; Preuss, H. Energy adjusted pseudopotentials for the actinides. Parameter sets and test calculations for thorium and thorium monoxide. *J. Chem. Phys.* **1994**, *100* (10), 7535−7542.
(54) Lee, C.; Yang, W.; Parr, R. G. Development of the Colle Salvetti correlation energy formula into a functional of the electron density. *Phys. Rev. B: Condens. Matter Mater. Phys.* **1988**, *37* (2), 785−789.
(55) Weigend, F.; Ahlrichs, R. Balanced basis sets of split valence, triple zeta valence and quadruple zeta valence quality for H to Rn: Design and assessment of accuracy. *Phys. Chem. Chem. Phys.* **2005**, *7* (18), 3297−3305.

(56) Klamt, A.; Schüürmann, G. COSMO: a new approach to dielectric screening in solvents with explicit expressions for the screening energy and its gradient. *J. Chem. Soc., Perkin Trans. 2* **1993**, No. 5, 799−805.
(57) Beele, B. B.; Rüdiger, E.; Schwörer, F.; Müllich, U.; Geist, A.; Panak, P. J. A TRLFS study on the complexation of novel BTP type ligands with Cm(III). *Dalton Trans.* **2013**, *42* (34), 12139−12147.
(58) Bremer, A.; Müllich, U.; Geist, A.; Panak, P. J. Influence of the solvent on the complexation of Cm(III) and Eu(III) with nPr BTP studied by time resolved laser fluorescence spectroscopy. *New J. Chem.* **2015**, *39* (2), 1330−1338.
(59) Skerencak, A.; Panak, P. J.; Hauser, W.; Neck, V.; Klenze, R.; Lindqvist Reis, P.; Fanghänel, T. TRLFS study on the complexation of Cm(III) with nitrate in the temperature range from 5 to 200 °C. *Radiochim. Acta* **2009**, *97* (8), 385−393.
(60) Breen, P. J.; Horrocks, W. D. Europium(III) luminescence excitation spectroscopy. Inner sphere complexation of europium(III) by chloride, thiocyanate, and nitrate ions. *Inorg. Chem.* **1983**, *22* (3), 536−540.
(61) Katzin, L. I.; Gebert, E. Spectrophotometric investigation of cobaltous nitrate in organic solvents. *J. Am. Chem. Soc.* **1950**, *72* (12), 5455−5463.
(62) Bünzli, J. C.; Vuckovic, M. M. Solvation of neodymium(III) perchlorate and nitrate in organic solvents as determined by spectroscopic measurements. *Inorg. Chim. Acta* **1984**, *95* (2), 105−112.
(63) Guillaumont, R.; Fanghänel, T.; Fuger, J.; Grenthe, I.; Neck, V.; Palmer, D. A.; Rand, M. H. *Chemical Thermodynamics (OECD NEA TDB)*; Elsevier: Amsterdam, 2003; Vol. *5*.
(64) Stephen, H.; Stephen, T. *Solubilities of Inorganic and Organic Compounds*; Pergamon Press: Oxford, London, New York, Paris, 1963; Vol. *1*, Part 1.
(65) Ewald, H. Die Analyse und Deutung der Neodymsalzspektren. *Ann. Phys.* **1939**, *426* (3), 209−236.
(66) Chodos, S. L.; Satten, R. A. Model calculation of vibronic sidebands in Cs_2UBr_6. *J. Chem. Phys.* **1975**, *62* (6), 2411−2417.
(67) Iben, I. E.; Stavola, M.; Macgregor, R. B.; Zhang, X. Y.; Friedman, J. M. Gd^{3+} vibronic side band spectroscopy. New optical probe of Ca^{2+} binding sites applied to biological macromolecules. *Biophys. J.* **1991**, *59* (5), 1040−1049.
(68) Trumm, M.; Wagner, C.; Schimmelpfennig, B.; Geist, A.; Panak, P. J. A closer look on the coordination of soft nitrogen donor ligands to Cm(III): SO_3 Ph BTBP. *Dalton Trans.* **2016**, *45* (31), 12308−12311.
(69) Weigl, M.; Geist, A.; Müllich, U.; Gompper, K. Kinetics of americium(III) extraction and back extraction with BTP. *Solvent Extr. Ion Exch.* **2006**, *24* (6), 845−860.

Trivalent actinide ions showing tenfold coordination in solution
— *Supporting Information* —

Patrik Weßling,*[,a,b] Tobias Schenk,[b] Felix Braun,[b] Björn B. Beele,[c] Sascha Trumm,[d] Michael Trumm,[a] Bernd Schimmelpfennig,[a,†] Dieter Schild,[a] Andreas Geist,[a] and Petra J. Panak[a,b]

[a] Karlsruhe Institute of Technology (KIT), Institute for Nuclear Waste Disposal (INE), P. O. Box 3640, 76021 Karlsruhe, Germany

[b] Ruprecht-Karls-Universität Heidelberg, Institut für Physikalische Chemie, Im Neuenheimer Feld 253, 69120 Heidelberg, Germany

[c] Bergische Universität Wuppertal, Inorganic Chemistry, Gaußstraße 20, 42119 Wuppertal, Germany

[d] Karlsruhe Institute of Technology (KIT), Center for Advanced Technological and Environmental Training (FTU), P. O. Box 3640, 76021 Karlsruhe, Germany

[†] Deceased: 09/13/19

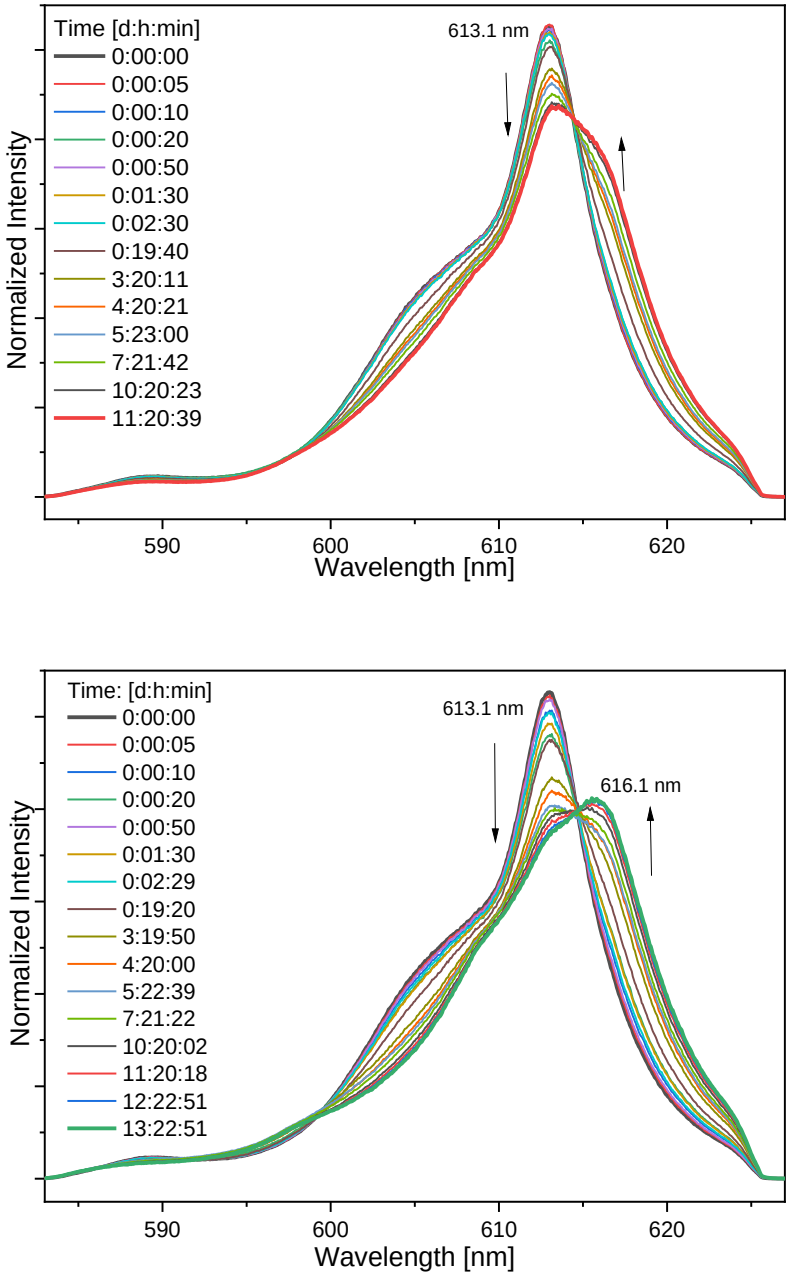

Fig. S1. Normalized Cm(III) emission spectra in 2-propanol containing 2.5 vol.% H_2O (top) and 5 vol.% H_2O (bottom) as a function of time after the addition of nitrate. $[Cm(III)]_{ini}$ = $1 \cdot 10^{-7}$ mol/L; [TBAN] = $4.03 \cdot 10^{-4}$ mol/L; [nPr-BTP] = $1.58 \cdot 10^{-5}$ mol/L.

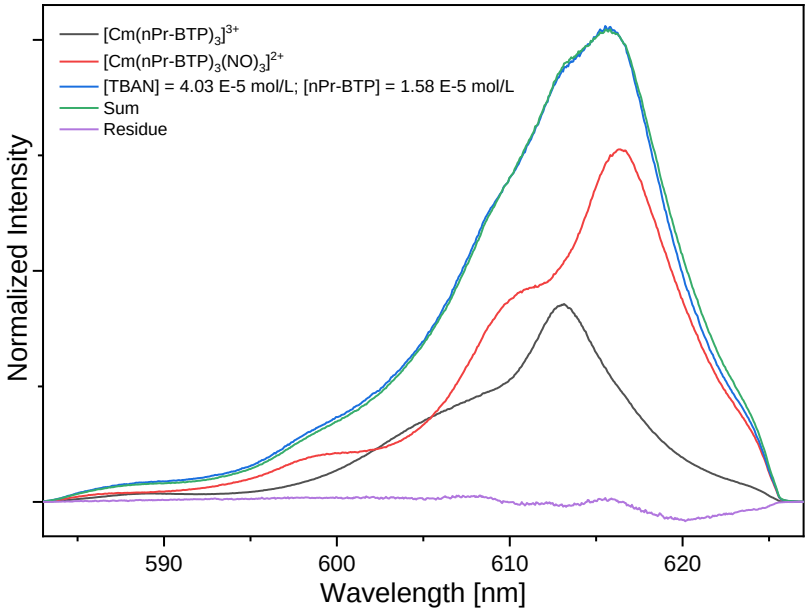

Fig. S2. Peak deconvolution of a Cm(III) emission spectrum in 2-propanol containing 5 vol.% H_2O. $[Cm(III)]_{ini}$ = $1 \cdot 10^{-7}$ mol/L; [TBAN] =$4.03 \cdot 10^{-5}$ mol/L; [nPr-BTP] =$1.58 \cdot 10^{-5}$ mol/L.

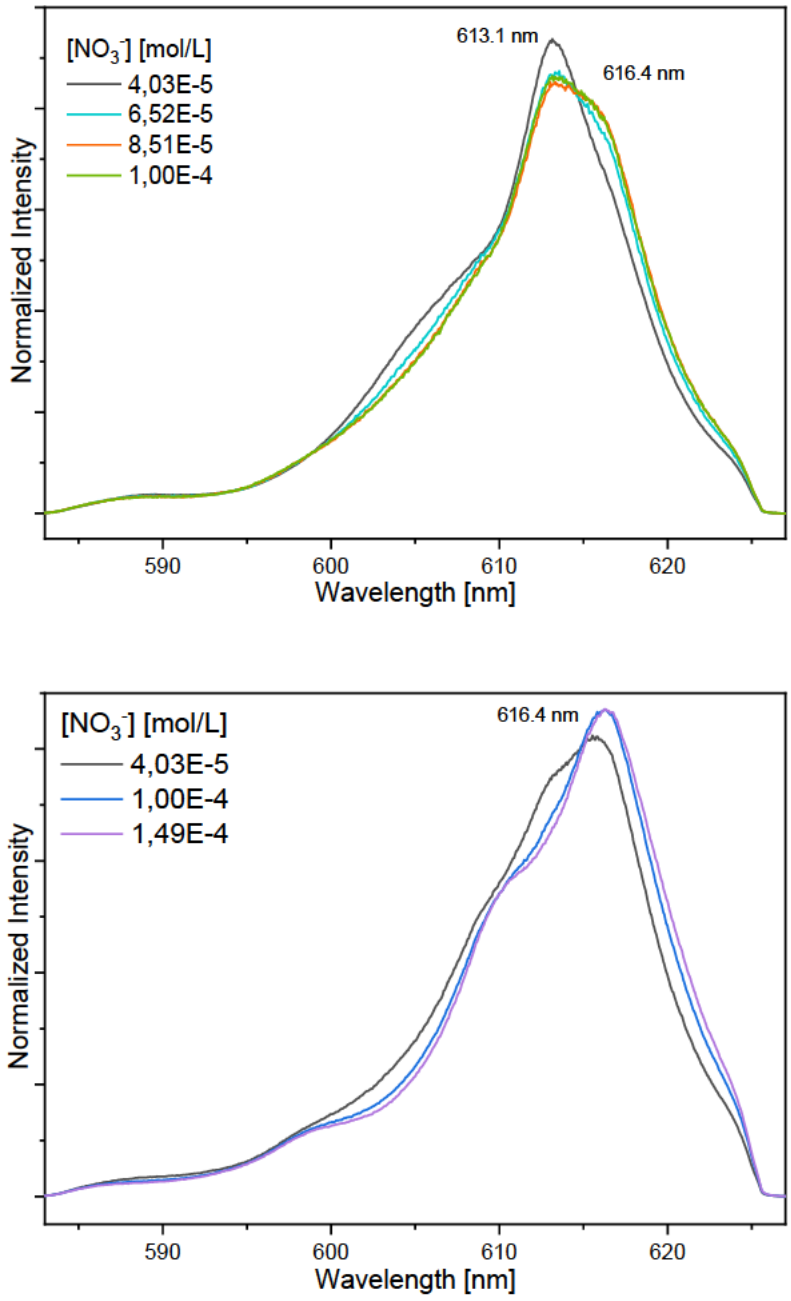

Fig. S3. Normalized Cm(III) emission spectra in 2-propanol (top) and 2-propanol containing 5 vol.% H_2O (bottom) as a function of the nitrate concentration. $[Cm(III)]_{ini} = 1 \cdot 10^{-7}$ mol/L; [nPr-BTP] = $1.58 \cdot 10^{-5}$ mol/L.

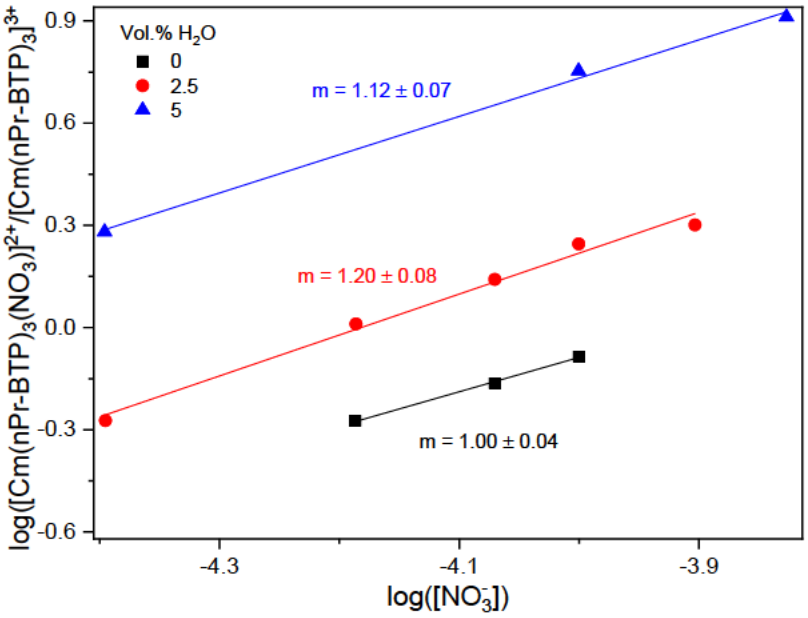

Fig. S4. Double logarithmic plot of the ratio of the molar fraction of species 1 and $[Cm(nPr\text{-}BTP)_3]^{3+}$ versus the nitrate concentration.

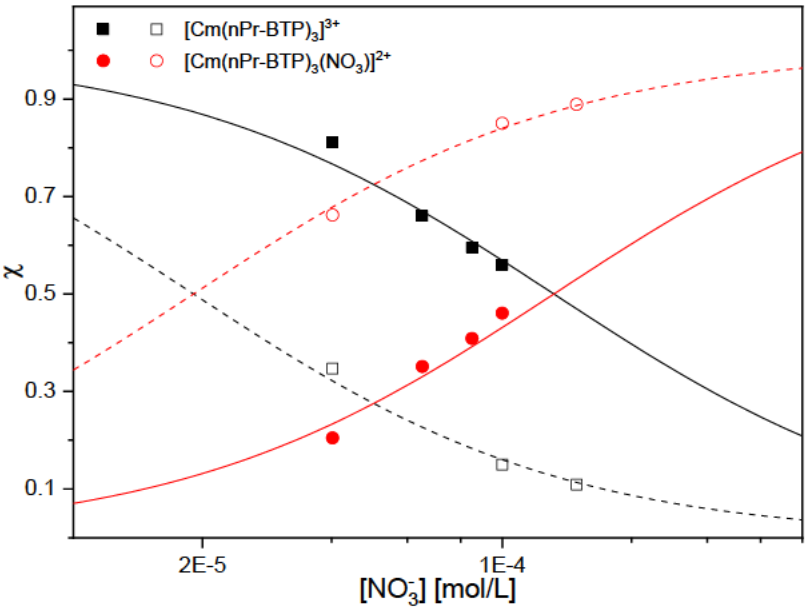

Fig. S5. Molar fractions of $[Cm(nPr\text{-}BTP)_3]^{3+}$ and $[Cm(nPr\text{-}BTP)_3(NO_3)]^{2+}$ in 2-propanol (closed symbols) and 2-propanol containing 5 vol.% H_2O (open symbols) as a function of the nitrate concentration. Lines are calculated with log β' = 3.9 (2-propanol, continuous lines) and log β' = 4.7 (2-propanol + 5 vol.% H_2O, dashed lines).

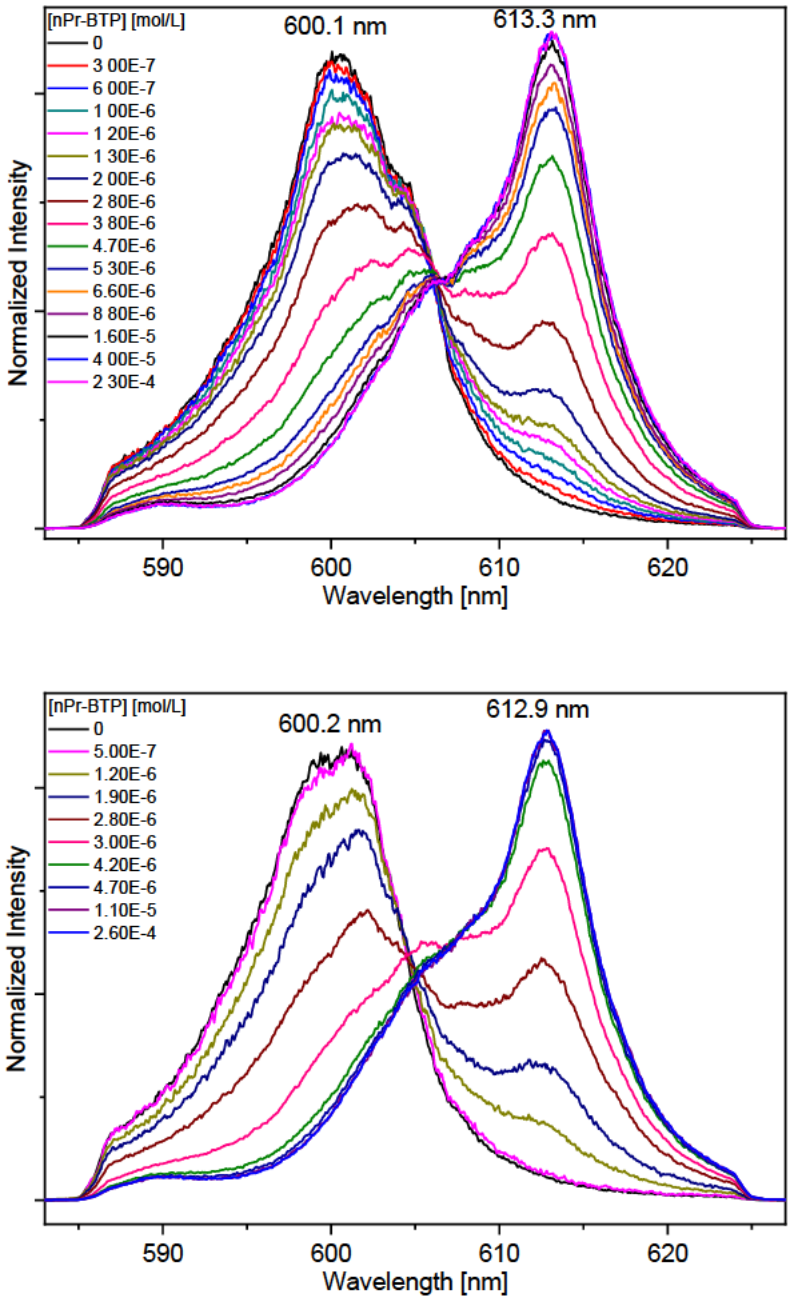

Fig. S6. Normalized Cm(III) fluorescence spectra as a function of the nPr-BTP concentration in methanol with constant cyanide (top) and triflate (bottom) concentration. $[Cm(III)]_{ini}$ = $2 \cdot 10^{-7}$ mol/L; $[CN^-] = [OTf^-] = 2 \cdot 10^{-5}$ mol/L.

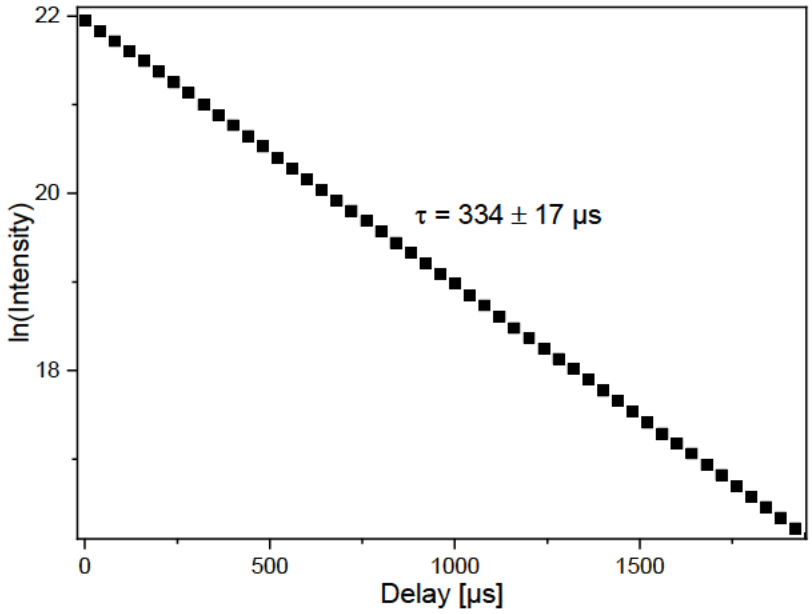

Fig. S7. Decay of the Cm(III) fluorescence intensity as a function of the delay time in 2-propanol with $1.6 \cdot 10^{-5}$ mol/L nPr-BTP and $4.03 \cdot 10^{-5}$ mol/L TBAN containing 2.5 vol.% H_2O. $[Cm(III)]_{ini} = 1 \cdot 10^{-7}$ mol/L.

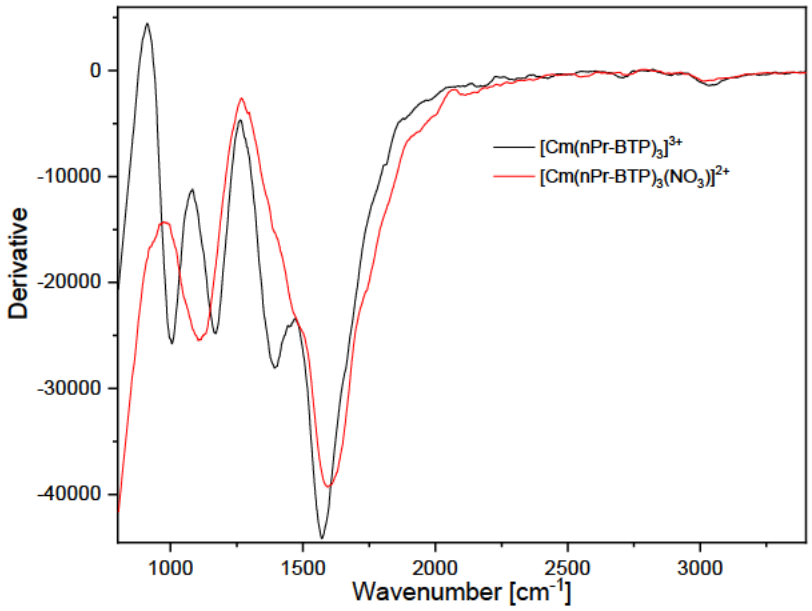

Fig. S8. Derivative of the VSB spectrum of $[Cm(nPr\text{-}BTP)_3]^{3+}$ in 2-propanol ($[Cm(III)]_{ini} = 1 \cdot 10^{-7}$ mol/L; [nPr-BTP] =$2.23 \cdot 10^{-5}$ mol/L) and VSB spectrum of a Cm(III) sample containing 64% $[Cm(nPr\text{-}BTP)_3(NO_3)]^{2+}$ in 2-propanol with 2.5 vol.% H_2O ($[Cm(III)]_{ini} = 1 \cdot 10^{-7}$ mol/L; [TBAN] = $1 \cdot 10^{-4}$ mol/L; [nPr-BTP] = $1.6 \cdot 10^{-5}$ mol/L).

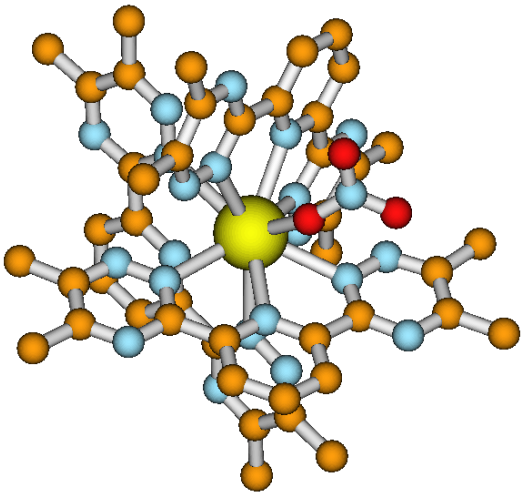

Position a

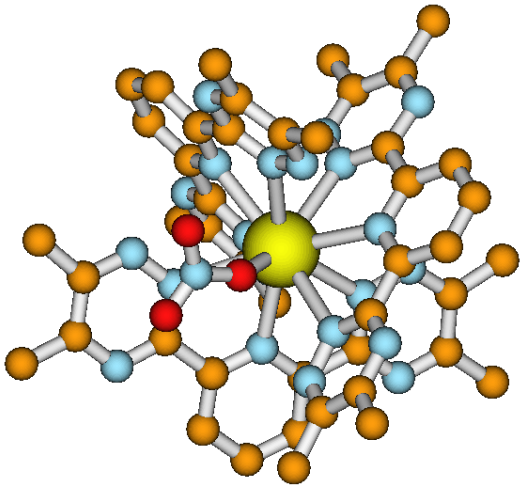

Position c

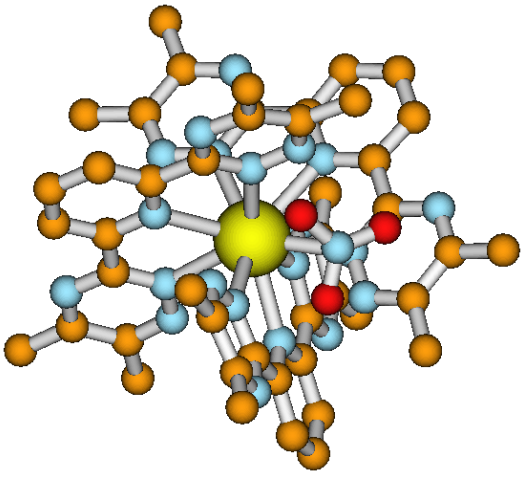

Position d

Fig. S9. Optimized structures of $[Cm(Me\text{-}BTP)_3(NO_3)]^{2+}$. Top, nitrate on the C_2 axis, short initial Cm-NO_3^- distance. Middle, nitrate ´on the C_3 axis, short initial Cm-NO_3^- distance. Bottom, nitrate on the C_3 axis, long initial Cm-NO_3^- distance. C, brown; N, blue; O, red; Cm(III), yellow. Hydrogen atoms omitted for clarity.

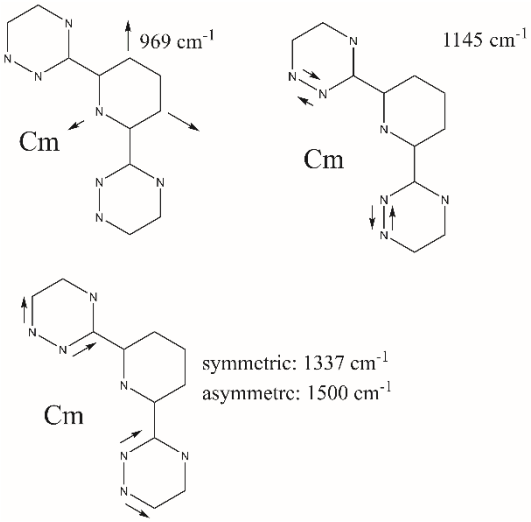

Fig. S10. Simplified representation of the vibrational modes of the BTP framework of $[Cm(Me\text{-}BTP)_3]^{3+}$ and $[Cm(Me\text{-}BTP)_3(NO_3)]^{2+}$.

	1	2	3
δ	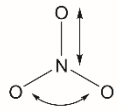	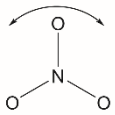	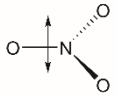
ν	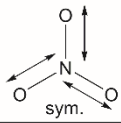	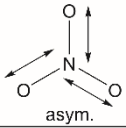	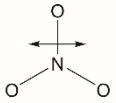

Fig. S11. Simplified representation of the NO_3^- vibrational modes in $[Cm(Me\text{-}BTP)_3(NO_3)]^{2+}$.

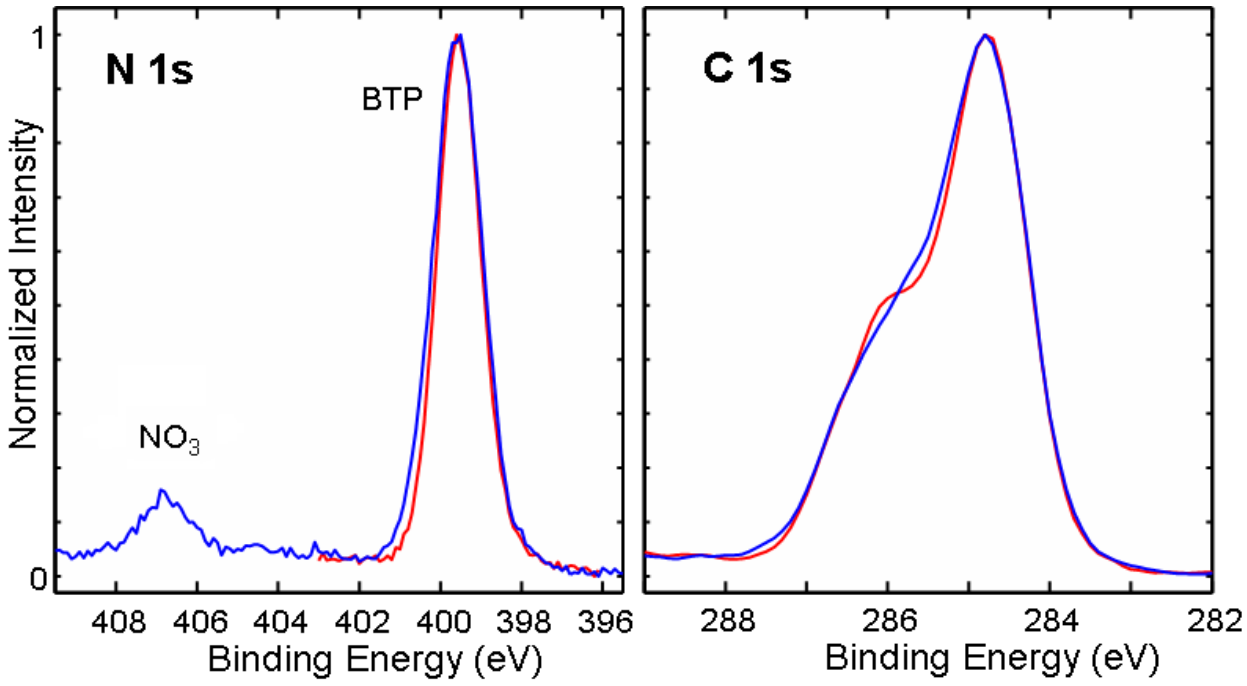

Fig. S12. N 1s (left) and C 1s (right) photoelectron spectra of nPr-BTP (red curve) in 2-propanol and nPr-BTP·HNO_3 (blue curve) in 2-propanol with 0.15 mol/L HNO_3. [nPr-BTP] = $3 \cdot 10^{-3}$ mol/L.

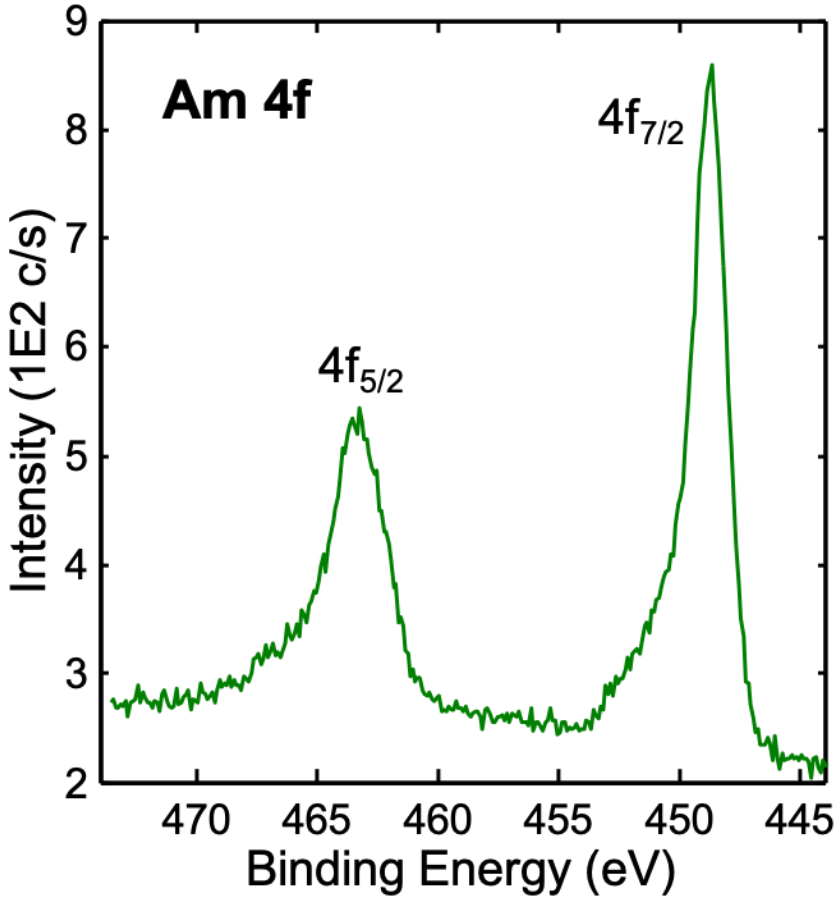

Fig. S13. Am 4f photoelectron spectrum of $[Am(nPr\text{-}BTP)_3(NO_3)](NO_3)_2 \cdot HNO_3$. The binding energy of Am $4f_{7/2}$ is 448.7 eV (FWHM 1.74 eV) and the 4f spin-orbit splitting 14.6 eV.